Macromolecular Bioscience
www.mbs-journal.de

Single Component Polymers, Polymer Blends, and Polymer Composites for Interventional Endovascular Embolization of Intracranial Aneurysms

*Hasan Hüseyin Karadeli and Emel Kuram**

Intracranial aneurysm is the abnormal focal dilation in brain arteries. When untreated, it can enlarge to rupture points and account for subarachnoid hemorrhage cases. Intracranial aneurysms can be treated by blocking the flow of blood to the aneurysm sac with clipping of the aneurysm neck or endovascular embolization with embolics to promote the formation of the thrombus. Coils or an embolic device are inserted endovascularly into the aneurysm via a micro-catheter to fill the aneurysm. Many embolization materials have been developed. An embolization coil made of soft and thin platinum wire called the "Guglielmi detachable coil" (GDC) enables safer treatment for brain aneurysms. However, patients may experience aneurysm recurrence because of incomplete coil filling or compaction over time. Unsatisfactory recanalization rates and incomplete occlusion are the drawbacks of endovascular embolization. So, the fabrication of new medical devices with less invasive surgical techniques is mandatory to enhance the long-term therapeutic performance of existing endovascular procedures. For this aim, the current article reviews polymeric materials including blends and composites employed for embolization of intracranial aneurysms. Polymeric materials used in embolic agents, their advantages and challenges, results of the strategies used to overcome treatment, and results of clinical experiences are summarized and discussed.

1. Introduction

An intracranial (cerebral) aneurysm is the abnormal focal dilation in brain arteries, which tend to be spherical in shape and weaken arterial blood vessels (**Figure** 1a,b).[1,2] Intracranial aneurysms can be critical and may remain undetected until the aneurysm ruptures and can cause hemorrhaging in the subarachnoid space surrounding the brain.[3] Incidental rupture of intracranial aneurysm is related to 50–80% of subarachnoid hemorrhages; it leads to death prior to medical attention and is related to a high mortality rate of up to 40% in the first week, accounting for ≈5–8% of all strokes.[4–10] When untreated, intracranial aneurysms can enlarge to rupture points and account for 50–80% of subarachnoid hemorrhage conditions. Owing to high morbidity and mortality related to rupture, early and efficient intracranial aneurysm therapy before rupture can raise the survival rate of the individual. Current common treatment techniques (Figure 1c) are clipping (**Figure** 2a) and endovascular embolization for blocking circulation into aneurysmal space to prevent aneurysm rupture.[2] Balloon, catheter, and coil methods have been added to equipment for endovascular therapy of cerebral arterial aneurysms (Figure 2b–d).[11] In the years from 1960s to 1980s, neuroendovascular concepts, neuroangiographic anatomy, balloons for intracranial usage, and micro-catheters of variable stiffness were precursors for endovascular therapy of intracranial aneurysms. The capability to repeatedly treat vasospasm allows the reduced mortality after endovascular or surgical therapy of intracranial aneurysm.[12] The development of detachable coils for aneurysm embolization has led to advances in endovascular balloon techniques in addition to endovascular coils.[11] Though positive outcomes are achieved with balloon reconstruction, some interventionists consider that balloon reconstruction does not reduce aneurysm recurrence rates and might be related to an increased incidence of thromboembolic events.[13] Balloon remodeling of wide-necked aneurysm is a significant adjunct to coil embolization, even in the acute phase. Acute subarachnoid hemorrhage secondary to wide-necked aneurysms is treated surgically. However, balloon remodeling has facilitated aneurysm therapy in the acute phase without the requirement of long-term antiplatelet therapy.[11] The

H. H. Karadeli[+]
Department of Neurology
Istanbul Medeniyet University Göztepe Prof. Dr. Süleyman Yalçın City Hospital
Istanbul 34722, Turkey
E. Kuram
Department of Mechanical Engineering
Gebze Technical University
Kocaeli 41400, Turkey
E-mail: kuram@gtu.edu.tr

The ORCID identification number(s) for the author(s) of this article can be found under https://doi.org/10.1002/mabi.202300432

[+]Present address: Medicana Ataköy Hospital, Stroke & Brain Aneurysm Center, Istanbul 34158, Turkey

DOI: 10.1002/mabi.202300432

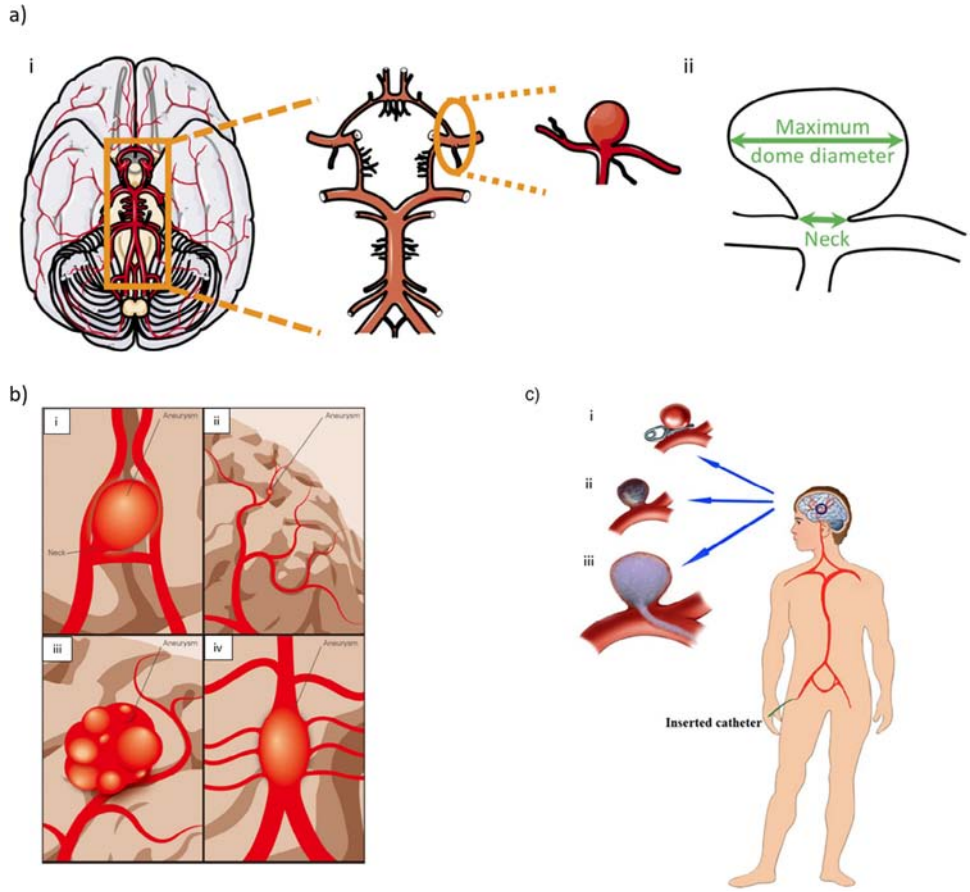

Figure 1. a) Cerebral aneurysm dome, from circle of Willis to histology. i) Location sample for aneurysm in the circle of Willis. ii) View for aneurysm dome. Measuring the location of neck size and maximum dome diameter is depicted. Reproduced under the terms of the CC-BY license.[19] Copyright 2021, The Authors. b) Types of intracranial aneurysm: i) Saccular: It resembles a rounded outpouching by aneurysmal domes and necks connecting with parent vessel. ii) Microaneurysm: It is an intracranial aneurysm less than 2 mm in diameter. iii) Giant: It is an intracranial aneurysm greater than 25 mm in diameter. iv) Fusiform: It is a widened and thinning segment of the artery. Reproduced under the terms of the CC BY 4.0 license.[20] Copyright 2017, The Authors. c) Treatment for cerebral aneurysm. i) Clipping. ii) Coiling. iii) Foaming. Reproduced under the terms of the CC BY 4.0 license.[21] Copyright 2021, The Authors.

promotion of stents in the early 2000s altered the management perspective of unruptured wide-necked intracranial aneurysms that could not be easily treated by coil embolization solely, with or without balloon, or with clipping.[11] The clipping requires craniotomy, an invasive surgery of the brain, after which a neurosurgeon embeds a clip along the aneurysm neck to block it from normal circulation (Figure 2a).[14] Clipping involves serious inherent risk to the patient. Also, clipping is not always feasible because of the inaccessible region of the aneurysm in the brain or patients with high risk for surgery because of age or related medical cases. Due to these limitations of clipping, endovascular treatment without open surgery has become an attractive option.[15] Embolization is a treatment in which some material is inserted to block the blood flow to a vessel defect, such as aneurysm, which is a swollen location on the artery wall.[16] Coils or an embolic device are inserted endovascularly into the aneurysm including fusiform, giant, and wide-necked aneurysms via a micro-catheter to fill the aneurysm (**Figure 3**a). This filling treatment involves isolating the weakened artery region from the rest of the vasculature and leads to endothelium regrowth, the artery's innermost layer over the entry point or aneurysm neck.[15] Endovascular therapy of intracranial aneurysm includes delivery and implantation of embolization coils in the aneurysm (Figure 3b) to promote the formation of thrombus and tissue healing (**Figure 4**).[17] It will decrease shear stress onto the weakened vessel and promote thrombosis with flow stagnation, speeding up healing.[18]

Several embolization materials have been developed, primarily for brain aneurysms that could cause rupture and fatal internal bleeding.[16] The first developed coil was indicated for peripheral embolization for vascular malformation and facial tumors. The coil was stiff, short in length, and did not involve specific shape memory, frequently causing difficulty in achieving complete occlusion of aneurysm.[11] The emergence of an embolization coil made of soft and thin platinum wire called the "Guglielmi detachable coil" (GDC) in 1991 could provide safer treatment for aneurysms.[25] Micro-catheter delivery endovascular treatment by GDC[25,26] is a less invasive surgery method aimed at excluding aneurysmal sac and neck from normal circulation through complete and lasting occlusion (**Figure 5**a–c). It is soft enough to fit into aneurysms without damaging the aneurysm wall.[27,28]

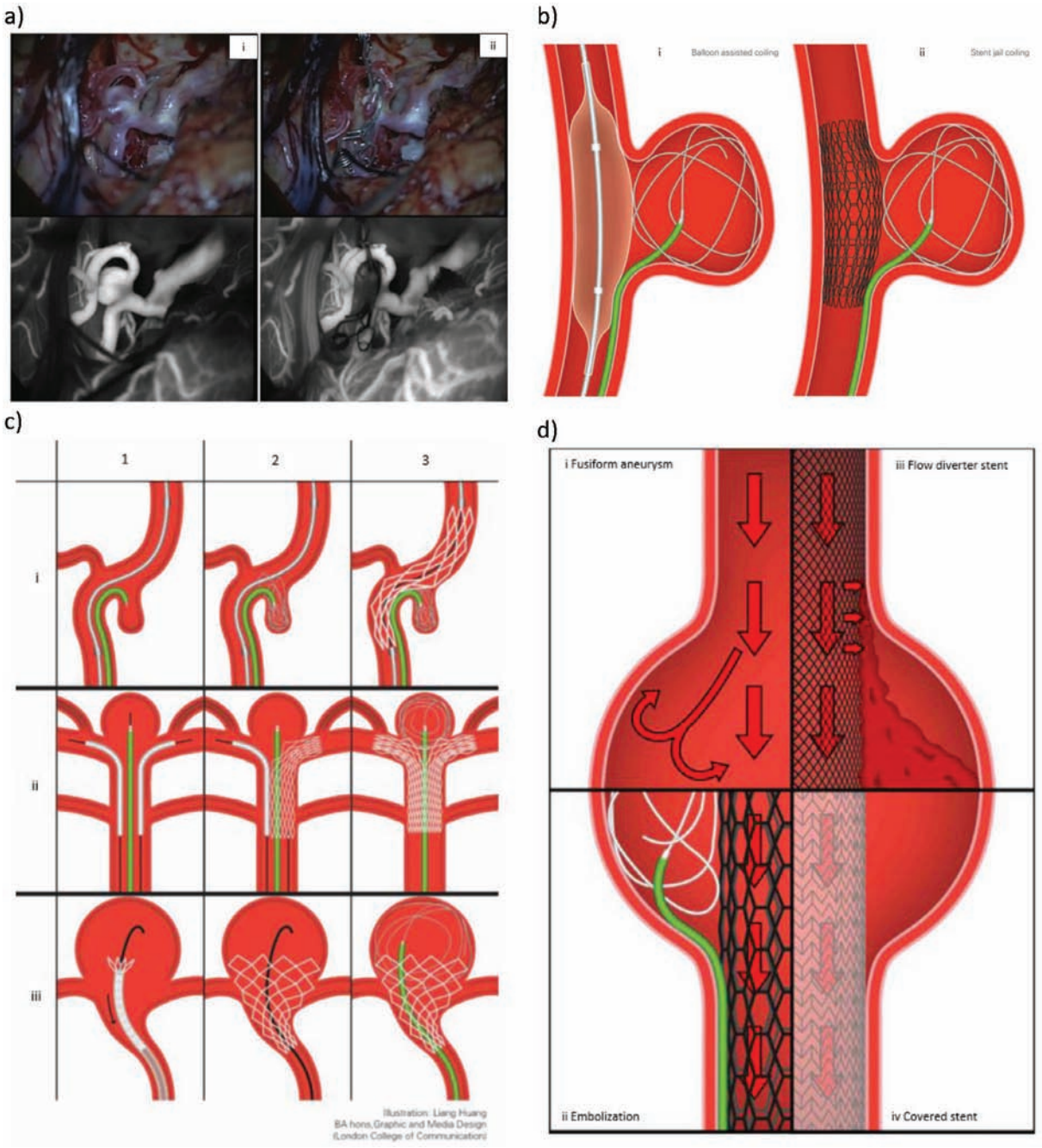

Figure 2. a) Intraoperative microscope-integrated near-infrared indocyanine green video angiography images prior to and after clipping (upper: microscope view; lower infrared visualization for blood flow). i) Middle cerebral artery (MCA) aneurysm before clipping. ii) MCA intracranial aneurysm after clipping. Reproduced under the terms of the CC BY 4.0 license.[20] Copyright 2017, The Authors. b) Schematic diagram of i) balloon-assisted coiling and ii) stent jail for wide-necked intracranial aneurysm. In balloon-assisted coiling, one or multiple nondetachable temporarily inflated balloons are used for blocking the aneurysmal neck during coil placement. In the stent jail method, the micro-catheter is placed prior to stent bridging over the aneurysmal neck. Reproduced under the terms of the CC BY 4.0 license.[20] Copyright 2017, The Authors. c) Schematic diagram of special stent-assisted techniques. i) Stent jack. i-1) Self-expandable stent navigated along aneurysmal neck and micro-catheter in aneurysmal sac. i-2) First coil deployed. i-3) Stent deployed fully (or partially) bridging neck, pushing coil in sac. ii) Y-stent. ii-1) micro-catheter navigated into sac whereas two neuroform stents navigated along basilar artery and respective posterior cerebral artery with exchange wires. ii-2) I stent deployed. ii-3) Contralateral stent deployed in "kissing" fashion. iii) Waffle-cone method. iii-1) Enterprise stent and exchange-wire positioned. iii-2) Stent deployed. iii-3) Micro-catheter positioned, coils deployed in waffle-cone configuration. Reproduced under the terms of the CC BY 4.0 license.[20] Copyright 2017, The Authors. d) Schematic view of treatment for fusiform intracranial aneurysm. i) Hemodynamics within a fusiform intracranial aneurysm. Turbulence forms because of the geometric shape of the fusiform intracranial aneurysm. ii) Stent-assisted coiling for fusiform intracranial aneurysm, requiring dense packing of coils. iii) Braided mesh stent of fusiform intracranial aneurysm. iv) Covered stent of fusiform intracranial aneurysm. Reproduced under the terms of the CC BY 4.0 license.[20] Copyright 2017, The Authors.

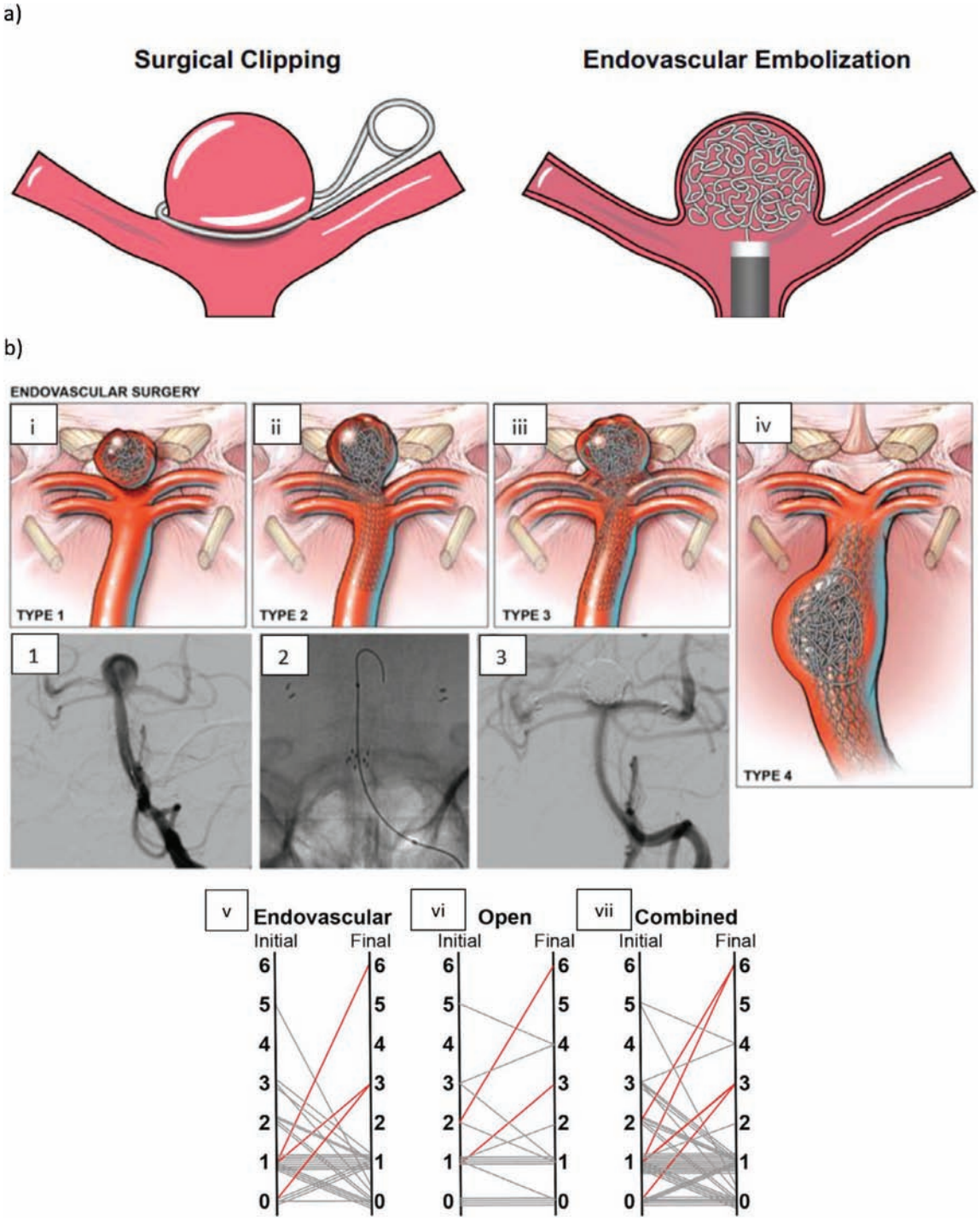

Figure 3. a) Schematic view of surgical clipping (clip not shown with scale) (left) and endovascular embolization employing GDC (right) for aneurysm treatment. Reproduced under the terms of the CC BY 4.0 license.[22] Copyright 2022, The Authors. b) Schematic views for endovascular interventions of basilar artery aneurysm. i–iii) The relationship between aneurysm neck and posterior cerebral artery (PCA) origin affects the choice of techniques for basilar tip aneurysm. i) Narrow-necked aneurysms with no involvement of proximal P1 origins are primarily coiled. ii,iii) Wide-necked aneurysms including one or both P1 origins are treated via one stent or two stents in Y configuration, respectively, to enable coil embolization. Inset (1, 2, 3) represents intraprocedural angiography showing optimum stent position and coil embolization causing complete aneurysm obliteration of wide neck basilar artery apex aneurysm (type 3). Injection, left vertebral. Projection, anterior-posterior. iv) In some basilar trunk aneurysms that can be circumferentially coiled to embolize saccular components, a micro-catheter is jailed via stent in the basilar trunk to keep luminal patency. Then, stent-assisted coiling is conducted. v–vii) Clinical outcomes (modified Rankin score, mRS) following endovascular and open surgery for basilar artery aneurysm. Left axis, pre-intervention mRS. Right axis, mRS at last follow-up. Red, clinically important mortality or morbidity. Gray, unaltered or enhanced disability. Reproduced under the terms of the CC BY 4.0 license.[23] Copyright 2021, The Authors.

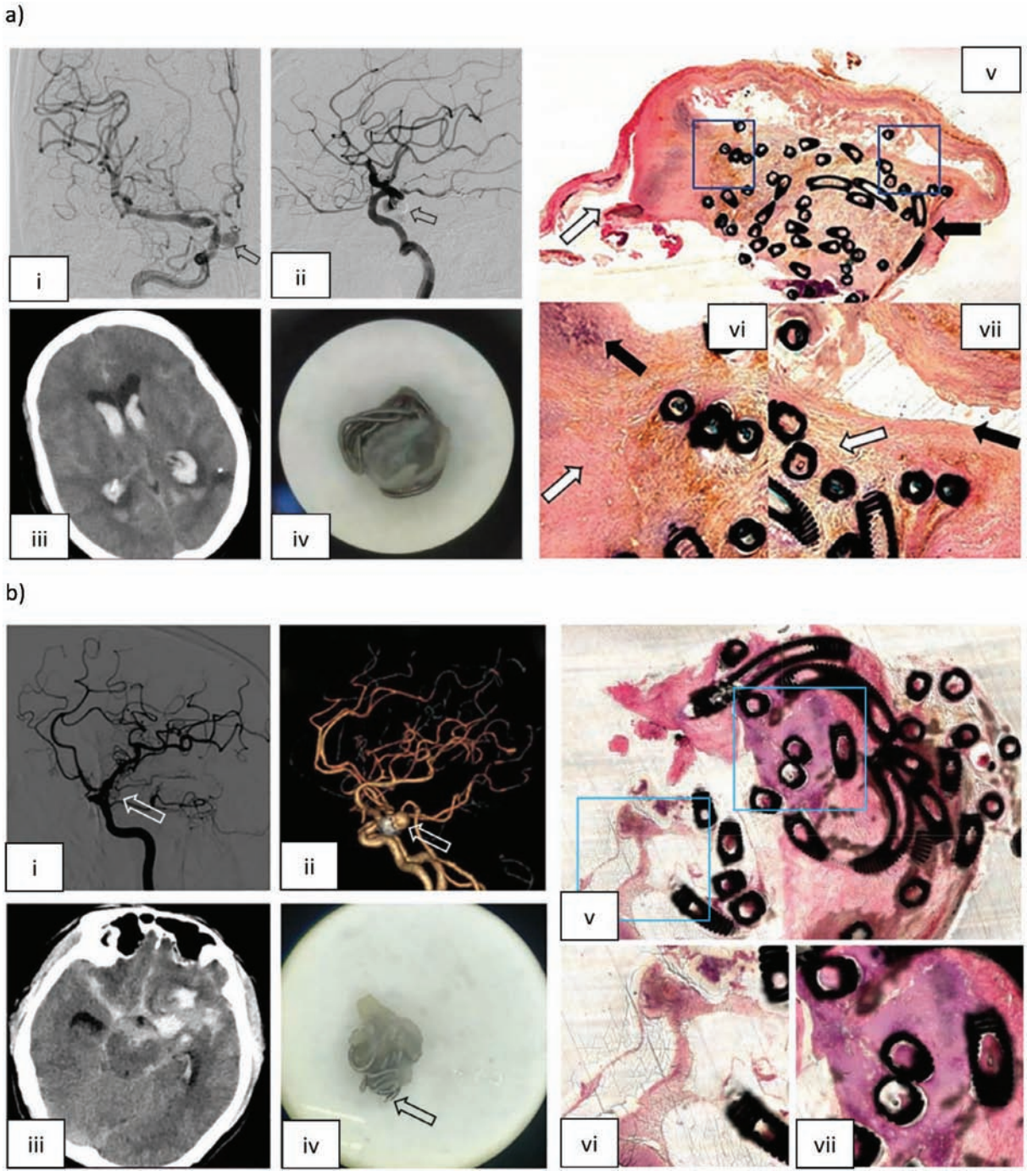

Figure 4. a) Patient with aneurysm in LC7. i) Angiography shows complete obliteration for aneurysm via stent-assisted coiling in the second therapy (open arrow). ii) Pre-clipping angiography demonstrates aneurysm recurrence (aneurysm growth and coil compaction of residual neck and subarachnoid hemorrhage) (open arrow). iii) Pre-clipping computed tomography (CT) demonstrates hemorrhage in the ventricle and fissures. iv) Gross sample with coils packed with thrombus and wall. v–vii) Microscopic section (hematoxylin-eosin stain, magnification ×4 and ×12.5). v) Empty space is observed near the aneurysm neck (open arrow), and coils are attached to the thrombus (arrow). vi) Granulation tissue (open arrow) composed of fibroblasts, infiltrating inflammatory cells, and thrombus (arrow). vii) Coils forming tight junctions with scar tissue (mature granulation) (open arrow), resulting in surface angiogenesis (endothelial cell formation) (arrow). Reproduced under the terms of the CC BY-NC 4.0 license.[24] Copyright 2022, The Authors. b) Patient with aneurysm in LC7. i) Digital subtraction angiography shows complete aneurysm occlusion in LC7 (open arrow). ii) CT demonstrates recanalization by aneurysm growth (open arrow). iii) CT demonstrates subarachnoid hemorrhage from aneurysm (linear high signal in basal cistern and longitudinal fissure, patchy heterogeneous high signal shadow in left frontal base, low signal ring around). iv) Gross sample having coils protruding from the aneurysm wall (open arrow). v–vii) Microscopic section (hematoxylin and eosin stain, magnification ×5 and ×12.5 indicating fresh thrombus loosely connected with coils (open arrow) and surrounding serum effusion and necrotic collagen fibers (arrow). Reproduced under the terms of the CC BY-NC 4.0 license.[24] Copyright 2022, The Authors.

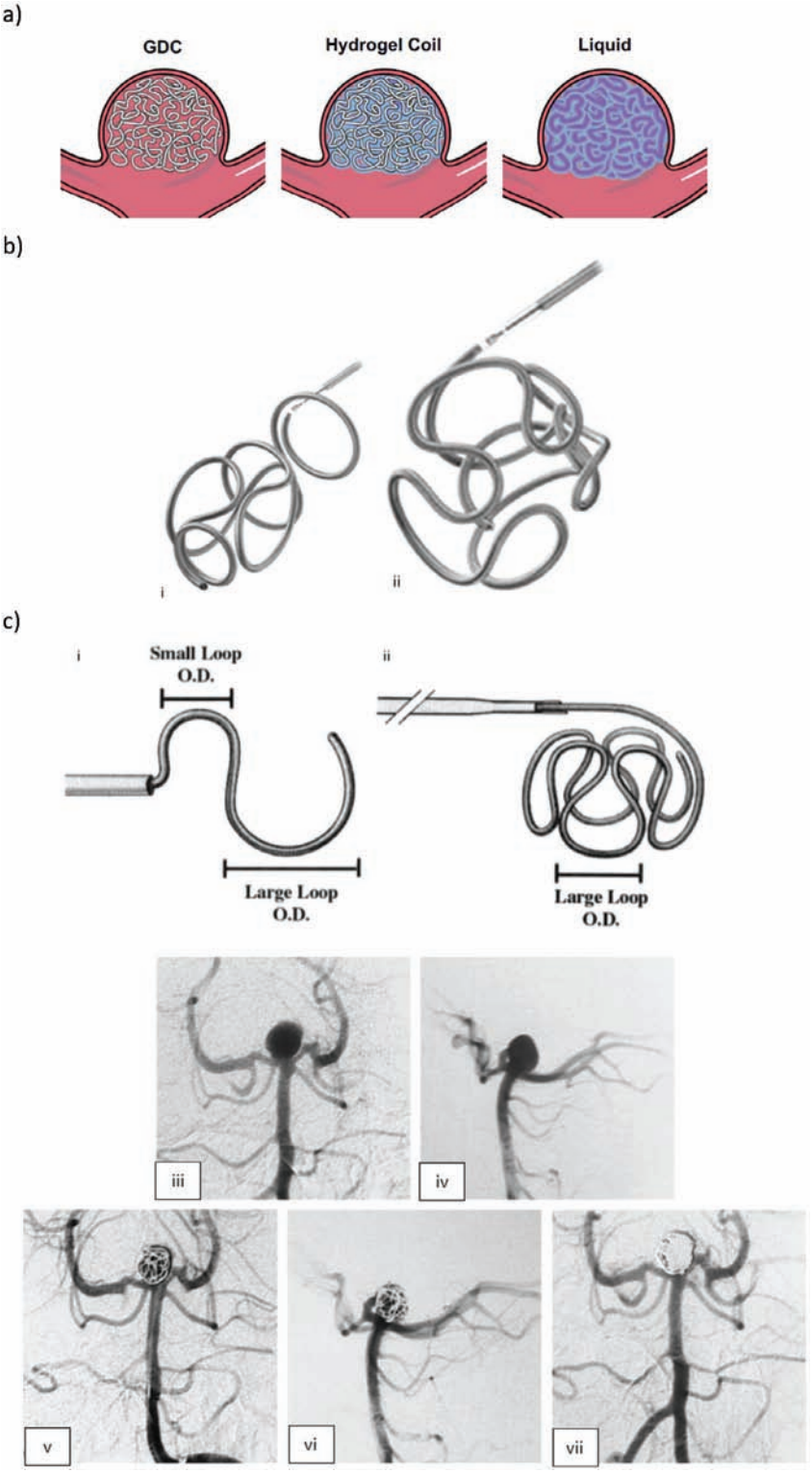

Figure 5. a) View for GDC, hydrogel coil, and liquid embolic devices. Reproduced under the terms of the CC BY 4.0 license.[22] Copyright 2022, The Authors. b) GDC coils. i) GDC 360° coil. ii) GDC 10 3D coil. Reproduced with permission.[46] Copyright, American Society of Neuroradiology. c) 3D GDC. i) Large and small loops alternate at 90° when it was deployed from the micro-catheter and ii) when fully deployed, forming a complex, spherical, 3D coil shape. Angiograms in a patient with basilar tip aneurysm treated via 3D GDC. iii) Anteroposterior projection demonstrates a wide-necked basilar aneurysm. iv) Lateral projection demonstrates basilar aneurysm. v) Anteroposterior projection after deployment of 3D GDC (8 mm × 25 cm) demonstrates no important extension of coil loops in the parent artery. vi) Lateral projection after deployment for 3D GDC. vii) Angiogram after placement for additional eight GDCs demonstrates complete aneurysm packing. Reproduced with permission.[47] Copyright, American Society of Neuroradiology.

Additionally, GDC can be separated from the delivery wire in aneurysm within minutes, making the embolization procedure quick and easy to use.[29] As in endovascular embolization, patients may face aneurysm recurrence because of incomplete coil filling or compaction over time.[30] Among the disadvantages of GDC, coil compaction is the most crucial. After embolization, internal pressure created with blood flow pushes the coil into compression, resulting in coil compaction, a major cause of recurrence and failure. It occurs when packing density (ratio for implanted coil volume to aneurysm volume) for GDC is small. The packing density for GDC is ≈30%, indicating that the remaining 70% must be filled by fairly thrombus.[31–34] Though GDC-based coil embolization treatment is an alternative to surgical clip ligation related to greater mortality,[35,36] some works[37–40] demonstrated that unsatisfactory recanalization rates and incomplete occlusion are drawbacks for endovascular embolization. So, the fabrication of new medical devices and methods for usage at less invasive surgical processes in accordance with the patient's complicated aneurysm shape is mandatory to enhance long-term therapeutic results for existing endovascular methods and to accomplish clinical difficulties declared here. In order to increase packing density for platinum coil, HydroCoil was developed where platinum one was wrapped by polymer hydrogel (Figures 5a, and 6a,b).[41] HydroCoil compared with bare GDCs concluded that the usage of hydrogel-coated coil reduced major aneurysm recurrence, but other clinical outcomes were comparable to the control group (i.e., bare GDC).[42,43] This later caused the development of HydroSoft, in which hydrogel was employed as an inner core (Figure 6c,d). HydroSoft intended to the decrease drawbacks of HydroCoil that introduced coil stiffness and greatly sensitive time constraints for delivery.[22] It was declared that the HydroSoft coil had a smaller rate of neck remnant (Raymond–Roy occlusion classification scale class II [RROC-II]) than HydroCoil.[44] Using ultra-low-density shape memory polymers (SMPs) instead of traditional platinum coils can give greater control and predictability to alleviate these complications.[2] Also, the SMP-coated coil increased packing density and enhanced tissue healing. Bulk packing density was computed as 37% without foam expansion and 92% with foam expansion.[45]

We have reviewed available studies and presented historical milestones in the development of neuroendovascular surgery for intracranial aneurysms. This article reviews polymeric materials employed for embolization. Polymers, SMPs, polymer blends, and polymer composites used in endovascular embolization of intracranial aneurysms are presented in detail under separate headings. Highlighted results obtained in studies using polymeric materials are summarized.

2. Single Component Polymers

The long-term durability question for platinum coil therapy has caused advances in various embolic devices. The developed devices often contain some kind of polymeric material to change the physical or biological properties of the implant, along with a platinum filament backbone for deliverability and radiopacity.[51] To overcome the drawbacks of platinum-based coil, some polymer embolization materials have been sought because they are expected to provide greater packing density and more rapid thrombus formation to block blood flow at a much lower cost. They are produced particles, liquids, or solutions forms for embolization. For endovascular therapy of cerebral aneurysm, polymeric embolization materials are present in the literature.[52–54] Alternative aneurysm filling materials include collagen-based coil,[55] hydrogel polymer,[56] hybrid metal and hydrogel coil,[57] SMP coil,[3] and polymer foam,[58] but not limited to those mentioned herein.

Several embolic polymers have been used in the treatment of intracranial aneurysms, including acrylics, muscle, silk, iron particulates, and hair.[12] The main drawbacks of these techniques include the unpredictable persistence of embolic polymer inside the aneurysm, as well as dangerous imaging modalities. The advent of biplanar angiographic imaging, balloons, catheters for enhanced intracranial flow, and most recently Onyx (MTI, Inc., Irvine, CA, USA) has caused version of balloon-assisted methods to intracranial aneurysm embolization.[11] In early 1990s, Kinugasa et al.[59,60] used cellulose acetate as an embolic agent in intracranial aneurysm therapy.[59,60] Cellulose acetate is thrombogenic and has a larger risk of leading to thrombosis. Even if the aneurysm is initially successfully obliterated via it, it may disappear, causing the aneurysm to be completely untreated.[61] Though an attractive method, polymer distal migration into the parent vessel was considered a complication for approach. Besides great density and relatively rapid polymer solidification, balloon assistance is needed in several cases. Polymer migration into the parent vessel is less likely if precautions are taken. Optimum micro-catheter performance is required to retain embolic polymer while giving moderate strength, traceability, and stability.[11] Yang et al.[62] concluded that cellulose acetate is not an ideal embolic for intracranial aneurysms as it severely damages vessels with a strong chemo-corrosive effect and might cause aneurysm rupture. Mordasini et al.[63] compared imaging characteristics of the polymeric coil with platinum one in vitro with an aneurysm model and in vivo with experimentally created rabbit carotid bifurcation aneurysm. Enhanced imaging quality with the usage of polymeric coil compared to platinum one was obtained.[63] Biocompatible poly(vinyl alcohol) (PVA) polymer in particle form was developed for embolization.[64] It was difficult to deposit PVA particles in the target aneurysm which led to side effects because of moving particles.[65] Silk-elastin-like protein polymer combines the solubility of mammalian elastin and silk strength. Silk-elastin-like was employed for embolizing aneurysms in a rabbit elastase model in vivo, obtaining > 90% occlusion and showing no cytotoxicity.[66]

An alternative procedure to coil or balloon methods proposed for the treatment of cerebral aneurysms is an embolic liquid that polymerizes or precipitates in situ upon contact with blood. The molecular weight of the polymer is a significant selection factor for embolic liquid, as only the greatest molecular weight homologues provide satisfactory embolization. Solvent viscosity, solvent-water mixture viscosity in injection region, and molecular weight of polymer need to be taken into consideration when preparing novel embolic liquid for cerebral aneurysm therapy.[67] Cyanoacrylate is representative of a liquid embolization agent. When in contact with blood, polymerization of cyanoacrylate occurs very rapidly, thus resulting in embolization to the target site. Polymerization frequently took place inside or at the catheter end, causing occlusion of the catheter or adherence of the catheter to the arterial wall.[68] Cyanoacrylate glue was

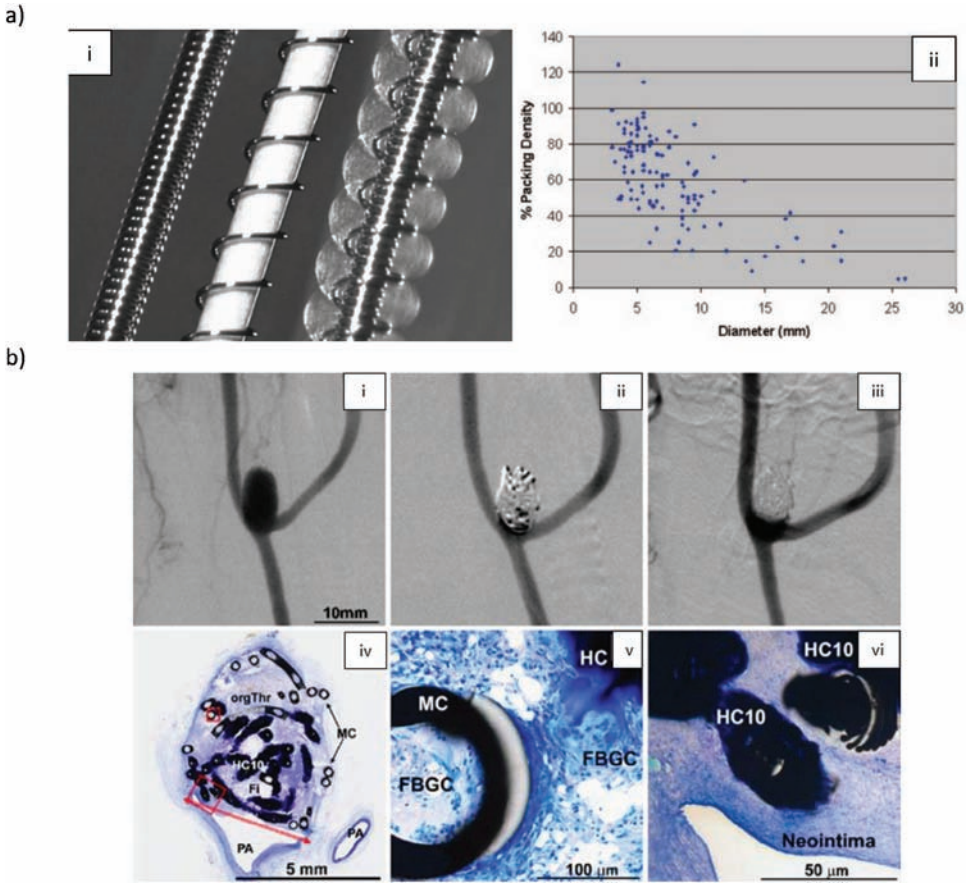

Figure 6. a–i) Hybrid hydrogel-platinum coil. Left, bare platinum coil. Middle, prehydration view demonstrates the initial profile of the device. Extremely compact hydrogel material is wrapped around a platinum coil. Outer "overcoil" is wrapped around a hydrogel-coated coil. The coil's outer diameter is 0.008 inches. Hydrogel thickness is about 0.0005 inches such that the gel coat outer diameter is 0.009 inches. The outer diameter with "overcoil" is 0.013 inches. Right, posthydration view of the device demonstrates a marked expansion of hydrogel, becoming translucent. The expanded hydrogel radial thickness is about 0.009 inches, such that the total outside diameter of the hydrated device is 0.027 inches. ii) Scatter plot of packing attenuation versus aneurysm diameter in aneurysm treated via the HydroCoil. HydroCoil gave relatively great packing attenuation, with an average of 60% and it reduced with the increment in aneurysm size. Reproduced with permission.[48] Copyright, American Society of Neuroradiology. b) Aneurysm treated via HydroCoil. i) Pre-embolization digital subtraction angiography (DSA), 4.8 × 9.5 mm (dome × length). ii) Post-treatment DSA, indicating a single loop protruding in the parent artery. iii) Follow-up DSA, indicating decreased neck contrast filling and no parent artery protrusion. iv–vi) Ground section, rapid bone stain surface staining. iv) Aneurysm overview, demonstrating platinum coil (MC) framing and HydroCoil 10 (HC10) filling at the sac center. HydroCoil was located toward the sac center. Note the organized red thrombus (orgThr) trapped in the dome and fibrin remnants (Fi) in the center. Coils protruding from the flat neck surface to parent arteries (PA) are not seen in this section. Enlarged top rectangle from (iv) demonstrating foreign body response (FBGC) to MC and HC10. vi) Enlarged lower rectangle from (iv) demonstrating thick neointima covering of HC10. Reproduced with permission.[49] Copyright 2009, Springer-Verlag. c–i) State of the HydroSoft coil before and after expansion. The platinum coil includes a hydrogel inner core and stretch-resistant filament. It expands and fills up to 40% more volume than the platinum coil. ii,iii) Enhanced occlusion degree. ii) Postembolization angiogram indicates residual filling into the aneurysm sac (arrow). iii) Seven-month follow-up angiogram demonstrates complete obliteration of aneurysm lumen (arrow). Reproduced with permission.[50] Copyright 2011, American Society of Neuroradiology. d) Aneurysm treated via HydroSoft. i) Pre-embolization DSA, 5.0 × 8.5 mm (dome × length). ii) Post-treatment DSA. iii) Follow-up DSA, indicating stable neck contrast filling. iv–vi) Ground section, rapid bone stain surface staining. iv) Aneurysm overview, demonstrating platinum coil (MC) framing, and HydroSoft (HySo) filling at the sac center. Flat neck surface at orifice plane, however, neointima-covered coils protrude into parent artery (PA). v) Enlarged top rectangle from (iv) demonstrating pronounced foreign body response (FBGC) to platinum overcoil and polymer filament (asterisk), however less to hydrogel of HydroSoft (HySo). vi) Enlarged lower rectangle from (iv) demonstrating HySo with FBGC underneath neointima. Reproduced with permission.[49] Copyright 2009, Springer-Verlag.

utilized as an embolic liquid for aneurysm occlusion, but its aggressive adhesive features could cause a "stick" of the catheter to the vessel.[69,70] Advantages and disadvantages of some liquid embolics used in aneurysm treatment are presented in **Table 1**.

A liquid, in situ gel polymer can be employed as an embolic agent for intracranial aneurysms. Liquid-to-solid gel properties can permit non-invasive endovascular delivery of material into aneurysms. Liquid embolic can be delivered non-invasively and provide a greater degree of aneurysm volume occlusion.[86] Important factors for the development of liquid embolics are biocompatibility, biodegradability, in situ setting time, mechanical properties, swelling, toxicity, viscidity, and viscosity.[92] ALGEL, an alginate-based embolic, was efficient in embolizing aneurysms in the swine model.[93,94] A great filling (≥ 93%) was

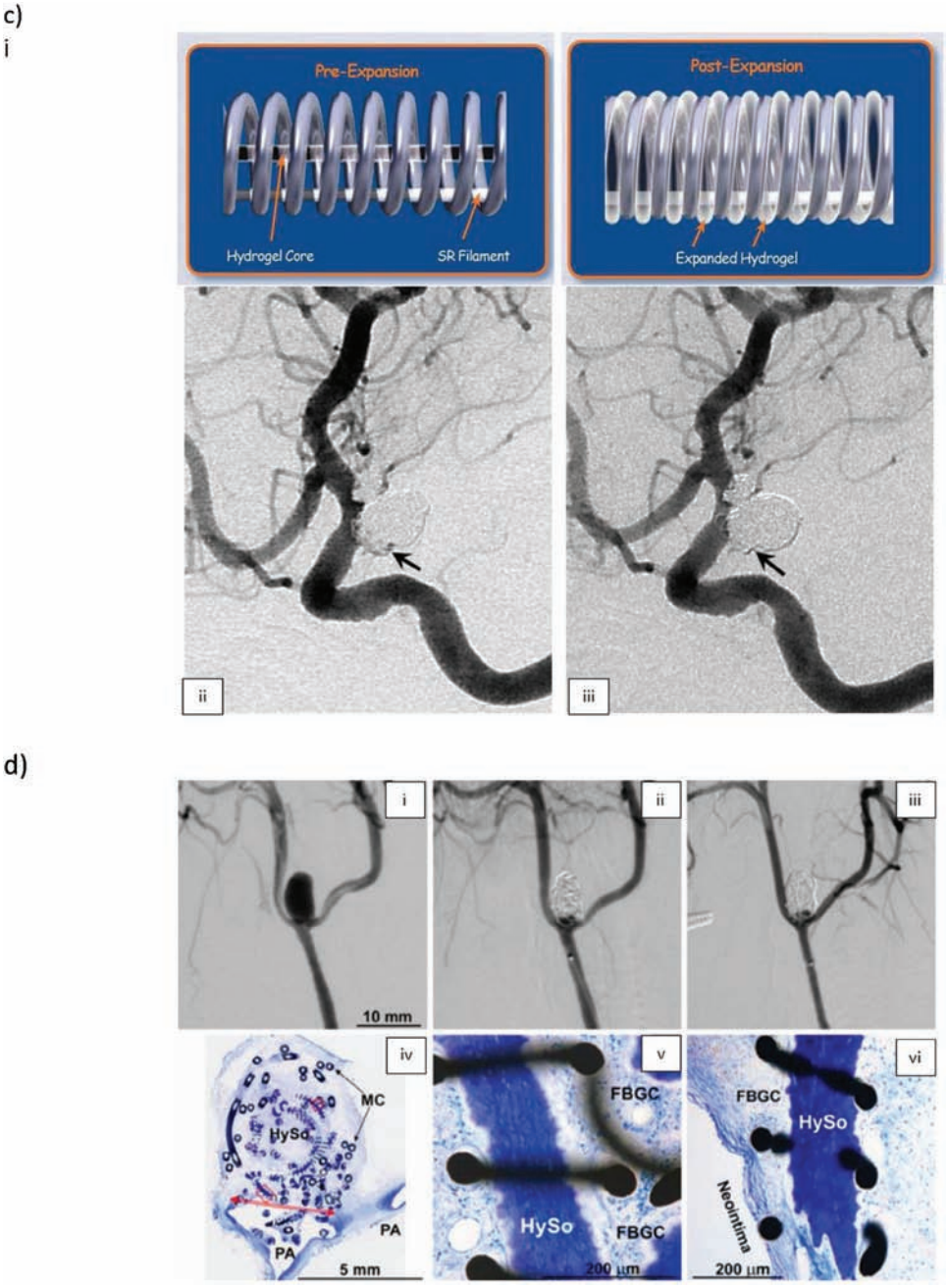

Figure 6. *Continued*

achieved by injecting ALGEL into the sac while the neck was blocked via a temporary balloon. Follow-up angiograms of work animals demonstrated that the parent vessel remained open, with the aneurysm remaining occluded after 90 days. Control animals with partially filled aneurysms lived only 6–8 days.[93] Safety concerns for alginate gel are material flow from the aneurysm cavity during administration, accidental embolization for non-target vessels, and alginate mass fracture after reintroduction of flow.[26] Takao et al.[95] developed thermoreversible gelation polymer as a novel embolic agent for endovascular therapy of experimental aneurysms created in bilateral common carotid arteries in swine. The material is original in that solidification takes place at physiological (body) temperature. Thermoreversible gelling polymer remains liquid at a temperature smaller than the sol-gel transition temperature (20 °C) and turns into a gelatinous solid greater than the sol-gel transition temperature. All aneurysms were successfully embolized with the new polymer but further modifications such as mechanical stability will be necessary before the clinical application of this polymer.[95] Calcium alginate gel has been employed in aneurysm occlusion. By simultaneously injecting calcium chloride and alginate into the sac, calcium alginate gel is created immediately in contact with two solutions.[94]

Table 1. Benefits and drawbacks of some liquid embolics utilized in aneurysms treatment.

Product	Benefits	Drawbacks	Reference(s)
Onyx PHIL	✓ Injectable liquid, allowing small vessel embolization. ✓ Non-adhesive. ✓ PHIL provided for usage in single syringe, inherently radiopaque.	× Material suspended in dimethyl sulfoxide (DMSO) demonstrated to result in vascular inflammation and angionecrosis. × Onyx needs multi-stage preparation via special tool. × Catheter entrapment may take place.	[71–90]
Iodine-containing PVA dissolved in *N*-methyl pyrrolidone (NMP)	✓ Not require any preparation prior to use (heating or shaking). ✓ Not require radiopaque mixtures. ✓ Artifact-free evaluation for aneurysms treated with multisection CT and magnetic resonance (MR) angiography. ✓ Employs NMP as solvent, which possesses low angiotoxicity	× From immediate results some complications (dissection, small leakage and lethal rebleeding) were observed. × From follow-up results mild and moderate inflammatory response were observed.	[91]

While this gel system presents good mechanical strength and biocompatibility features, emboli from unstable calcium alginate might occur in the parent artery, incomplete embolization might form, and instability may cause gel fracture.[26] Also, a couple of lumen catheter used for simultaneous injection of calcium chloride and alginate needs a higher size catheter and coordination in synchronized injection of both materials in the sac. Therefore, additional development is required in the area of liquid embolic for aneurysm occlusion.[96] Chen and Taguchi[97] prepared injectable inclusion complexes with α-cyclodextrin (α-CD) and hydrophobically modified PVA (hm-PVA) by different alkyl chain lengths (C3, C9, C18) as an embolization material not employing organic solvent at composition for the treatment of cerebral aneurysm (**Figure** 7a,b). hm-PVA (5% mol nonanal-modified PVA) with 15 mM α-CD gave moderate thixotropic features and the complex demonstrated gel-sol transition at various strain values (1% and 1000%). Lipids in the blood can facilitate gelation of α-CD/5% mol nonanal-modified PVA inclusion complex and improve its stability. After injecting α-CD/5% mol nonanal-modified PVA inclusion complex in an in vitro model produced by silicone rubber and glass plate, it caused aggregates in phosphate buffer solution (PBS) at 37 °C and completed the entire space (Figure 7c). Therefore, this inclusion complex can be a promising material for the treatment of cerebral aneurysms due to good injectability.

Alternative aneurysm embolic material appears in hydrogel form since they could be injected in liquid phase and solidified in situ. Hydrogel has the capability to fill aneurysm sac completely than solid implants such as that employed for coil embolization (**Figure** 8a).[98] Hydrogels should entirely fill the aneurysm, show long-term stability, not protrude or migrate in the parent vessel, and match the mechanical features of the aneurysmal wall to the surrounding native tissue (Figure 8b).[99] For hydrogel to be employed in vivo, degradation and swelling must be considered. Controlling swelling characteristic of hydrogel is significant in endovascular embolization of aneurysms. If hydrogels undergo creep deformation due to viscoelastic behavior in vivo, this can eventually result in the gel leaking into the parent vessel, causing further complications. Therefore, the drawbacks of hydrogel can be decreased via synthesis.[96] The potential risks of hydrogels are depicted in Figure 8c. Volume ratio and swelling pressure of hydrogels are important parameters. As aneurysm rupture could take place when wall stress passes tissue strength, hydrogel swelling and expansion should be sufficient to complete the cavity, as little as possible to avoid applying great pressure to the aneurysmal wall or protruding into the parent artery to prevent thromboembolic complication (Figure 8c).[98] Early hydrogel deformation, degradation, or shrinkage might favor aneurysm recurrence,[100] underlining the importance of the polymer withstanding continuous dynamic biomechanical load associated with pulsatile blood flow.[101] Elasticity, compliance, and hydrogel strength should match with the parent artery.[102,103] Maintaining the original shape, mechanical properties, and weight of hydrogel is critical to obtaining long-term outcomes.[104] Poupart et al.[98] developed liquid poly(ethylene glycol) dimethacrylate (PEGDMA, 10, 15, and 20 wt%) precursor at various molecular weights (2, 6, and 20 kDa) with the potential to be delivered to in vitro intracranial aneurysm model and to be photopolymerized employing UV light in situ. The material shows potential in vitro applications because of ease of usage and small erosion rate.[98,105] Swelling ratio increased by polymer content and molecular weight. When polymer content was increased, the mechanical properties (compressive elastic modulus, failure stress) of hydrogels increased. PEGDMA hydrogels with a molecular weight of 6 kDa at a 15% concentration appeared suitable to withstand continuous interactions with blood flow. Under pulsatile flow in in vitro model for 1 month, hydrogels demonstrated complete occlusion, stability, and integrity because of preservation of weight, mechanical features, and shape notwithstanding slight surface erosion, minimum swelling volume preventing protrusion of parent artery, and small swelling pressure that limits the stresses implemented on the aneurysmal wall; and elastic modulus and compliance that covered native aneurysm tissue range. In vivo works are essential to determining the long-term integrity and stability of hydrogel.[98]

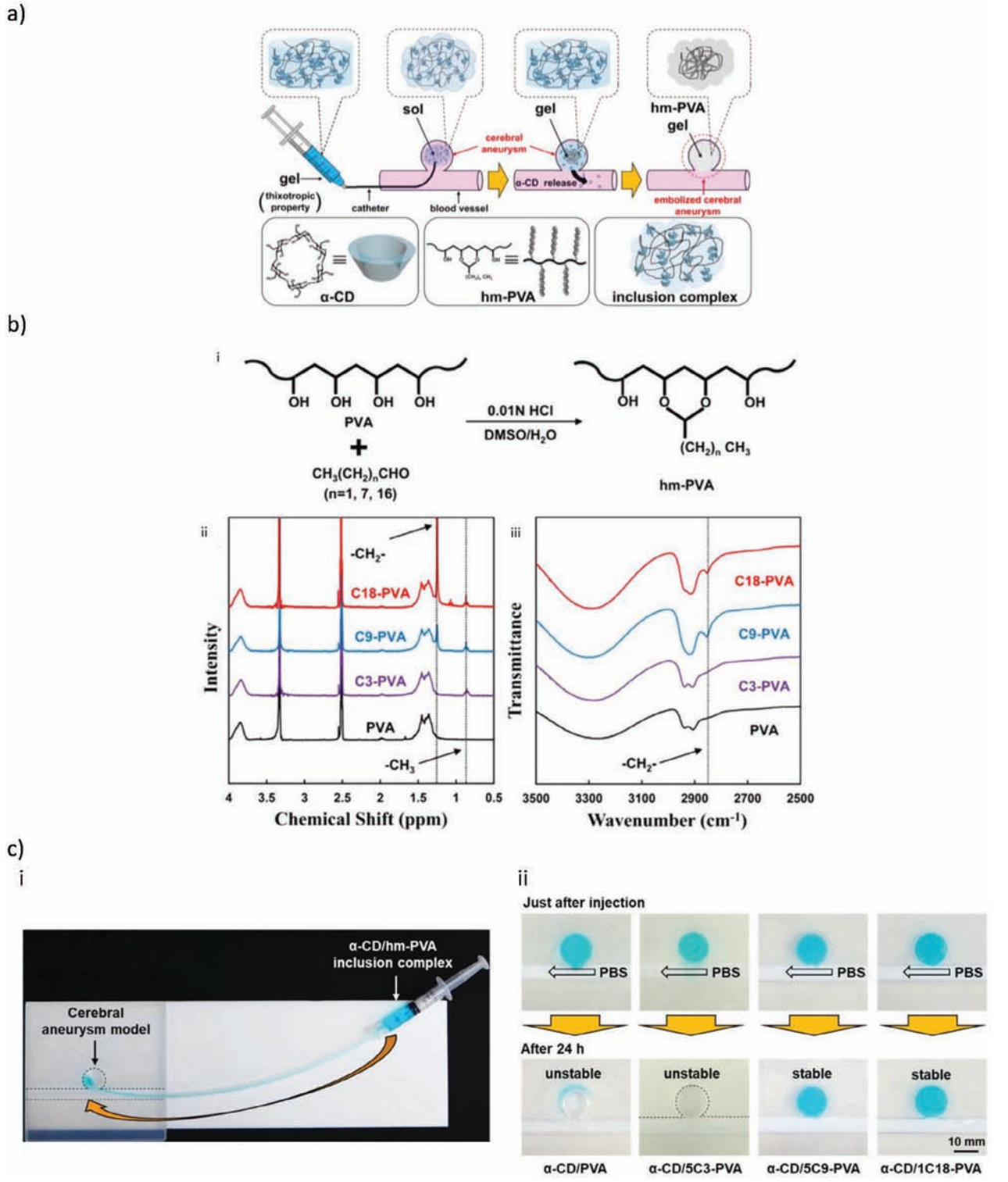

Figure 7. a) Schematic view of aneurysm embolization employing α-CD/hm-PVA inclusion complex. This inclusion complex having thixotropic features could be injected into the aneurysm via a catheter. Owing to physical crosslinks recovery (hydrophobic and hydrogen bond interactions), α-CD/hm-PVA inclusion complex could complete aneurysm. At last, stable hm-PVA gel made possible aneurysm embolization after α-CD release. Reproduced with permission.[97] Copyright 2020, The Society of Polymer Science, Japan. b) Synthesis and characterization for hm-PVAs. i) hm-PVAs synthesis. ii) ^{1}H-NMR for hm-PVAs. iii) FT-IR spectra for hm-PVAs. Reproduced with permission.[97] Copyright 2020, The Society of Polymer Science, Japan. c) Embolization for aneurysm model with α-CD/hm-PVA. i) Injection for α-CD/hm-PVA inclusion complex in aneurysm model. ii) Stability for α-CD/hm-PVA inclusion complexes having various alkyl chain lengths in PBS after incubation at 37 °C for 24 h. Reproduced with permission.[97] Copyright 2020, The Society of Polymer Science, Japan.

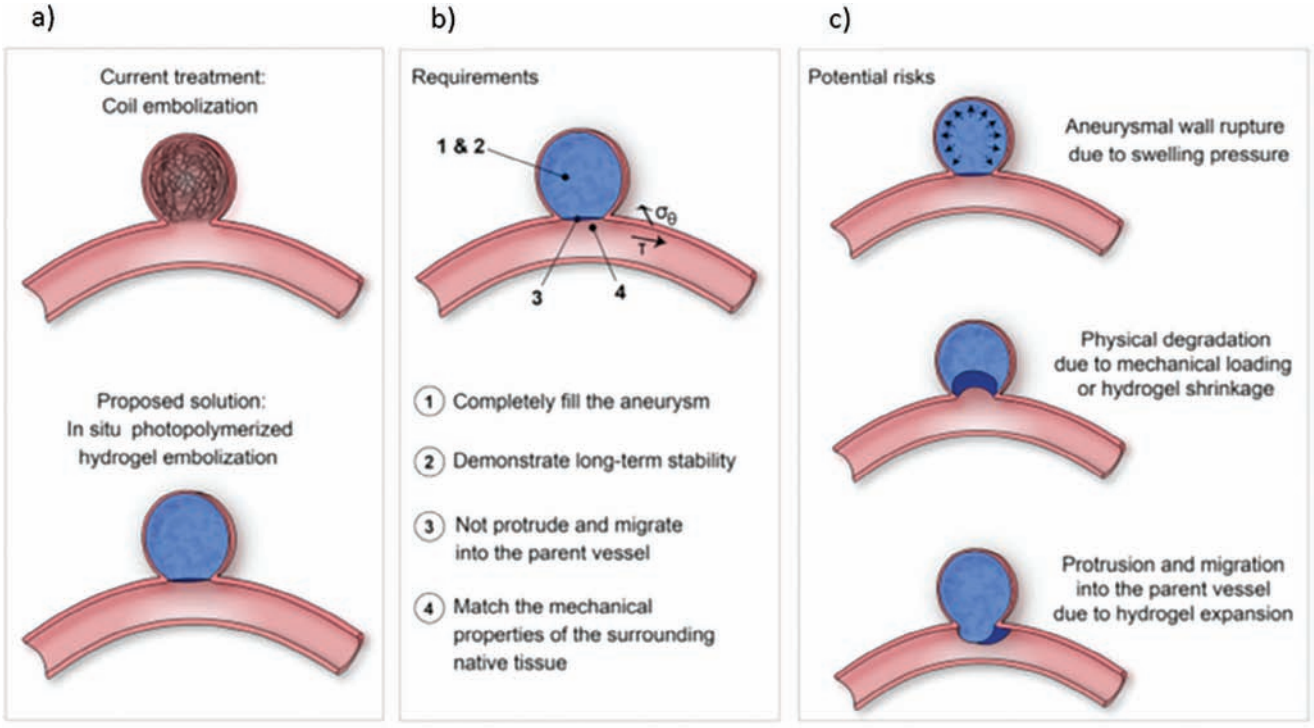

Figure 8. a) Suggested solution to use in situ photopolymerized hydrogel in embolization in place of coil. Reproduced under the terms of the CC BY license.[98] Copyright 2021, The Authors. b) Requirements. Reproduced under the terms of the CC BY license.[98] Copyright 2021, The Authors. c) Risks that such a solution needs to be evaluated. Reproduced under the terms of the CC BY license.[98] Copyright 2021, The Authors.

To overcome the drawbacks of platinum coils, second-generation coils, consisting of polymer in coating or filament form incorporated into platinum coil, have been fabricated.[106] Xu et al.[107] fabricated coil-in-shell device consisted of a metal coil (nitinol wire) surrounded with elastic biocompatible polymer [hyaluronic acid (HA) with polyurethane (PU) copolymer] shell, and tested in in vitro saccular aneurysm model and in vivo porcine aneurysm model. Both in vivo and in vitro works showed that developed coil-in-shell devices might be attractive in some cases as alternatives for conventional coil techniques, enabling more precise and controlled occlusion.[107] Hydrophilic polymers of different compositions have been implemented as coatings for endovascular devices to facilitate navigating within tortuous vessels, reduce endothelial trauma, and decrease thrombotic phenomena during the procedure.[108] Improving biological activity for the platinum coil can promote thrombus organization and accelerate endothelial cell proliferation.[109] Polymeric materials can be used in surface modification method of coils for intracranial aneurysm treatment. Coils containing filaments reduce flow across the aneurysm neck, increasing aneurysm occlusion.[110] Cerecyte bioactive coils contain a polyglycolic acid (PGA) filament within the lumen of the platinum coil. Its volume does not alter when PGA degrades. Another benefit of coils is their mechanical features.[111] Works about Cerecyte coils were more hopeful than other bioactive coils and demonstrated similar complication rates and enhanced durability in comparison to bare platinum coils.[111–114] In vitro thrombogenicity of platinum coils containing nylon and polyglycolic/polylactic acid (PGLA) filaments was evaluated, and it was concluded that these polymeric filaments increased thrombogenicity of the coil (**Figure 9**a,b). Nylon filament exhibited much greater thrombogenicity than PGLA filament (Figure 9c).[106] Q. Wang et al.[115] developed bioactive coil coating by poly(D,L-lacticide)−7co-(1,3-trimethylene carbonate) (P(DLLA-co-TMC) and the efficiency of the coil was evaluated by carotid artery aneurysm model in rats. Platinum coils were developed via sequential coating by anionic heparin and cationic P(DLLA-co-TMC). Next, recombinant human VEGF-165 (rhVEGF) was immobilized with binding affinity to heparin. It was found that P(DLLA-co-TMC)/rhVEGF-coated platinum coil could enhance clot organization and endothelial cell proliferation in the aneurysm model. However, further animal tests should be conducted to provide long-term safety for P(DLLA-co-TMC) during degradation into blood vessels.[115] cPax aneurysm therapy (NeuroVasx, Maple Grove, MN) is composed of a polymer strand that could be delivered by micro-catheter and detached at any point across the device length. The system is US Food and Drug Administration (FDA)-approved for cerebral aneurysms higher than 10 mm in diameter.[116] The hydrogel-coated coil was developed to reduce the amount of coil required to completely fill the aneurysm and to ensure increased coil packing.[11]

In summary, to overcome the drawbacks of today's endovascular methods, the optimum embolic agent should completely fill aneurysms, show long-term stability, not protrude or migrate in the parent vessel, and match the mechanical features of the aneurysmal wall to the surrounding native tissue.[99] The methodology and clinical outcomes of common polymeric materials employed in endovascular embolization procedures are presented in **Table 2**.

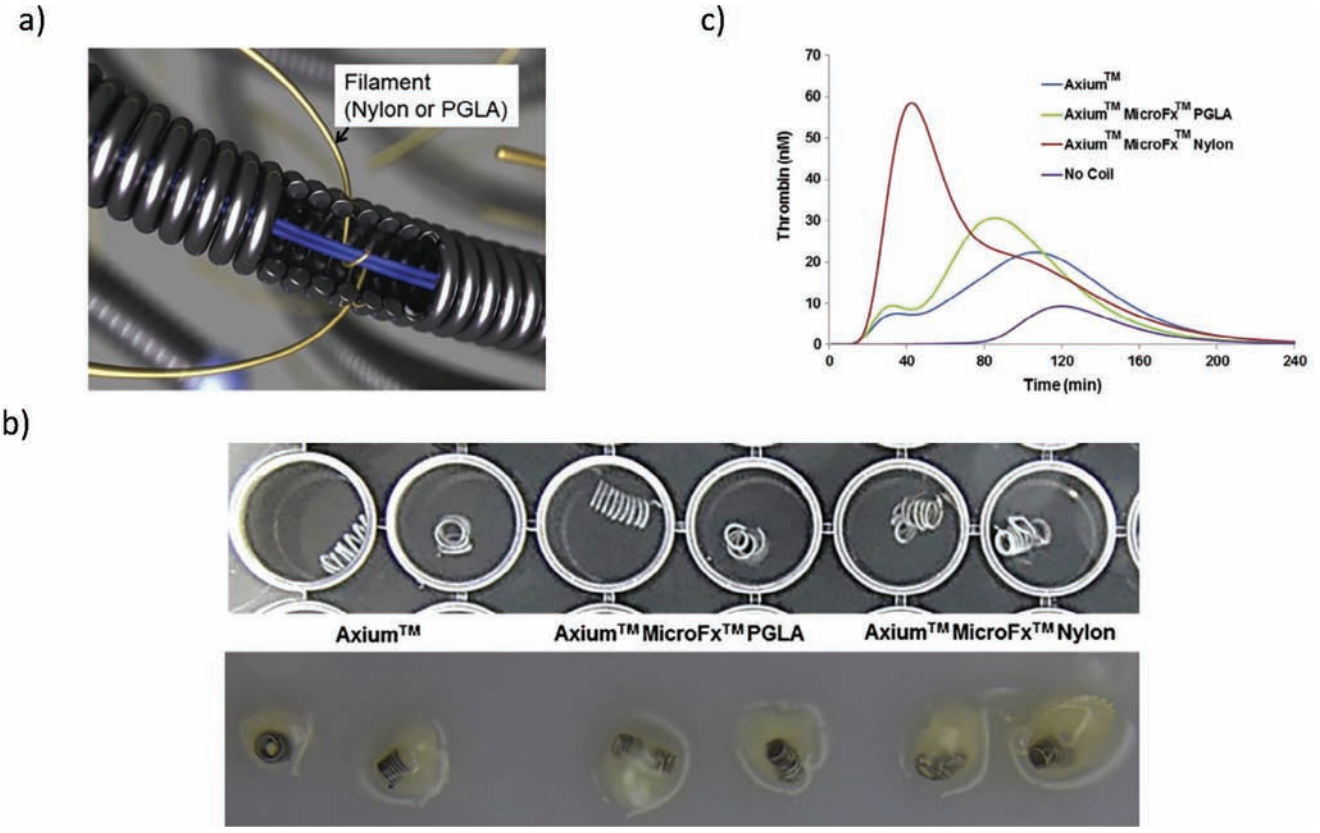

Figure 9. Axium MicroFx coil and post-experimental thrombus. a) Representation for Axium MicroFx coil section. All coil kinds used the same metallic chassis consisting of platinum alloy. The difference was that PGLA or nylon filament was added to Axium MicroFx PGLA and Axium MicroFx nylon coil. Reproduced with permission.[106] Copyright 2014, Elsevier B.V. b,top) Coils arrangement in a 96-well polystyrene microplate. Coil deployed in a random direction. b, bottom) Greater thrombus volume was found for filament-modified coil at the experiment end. Reproduced with permission.[106] Copyright 2014, Elsevier B.V. c) Thrombogram of thrombogenicity results for Axium and Axium MicroFx coils. Greater thrombin (peak thrombin, thrombin rate, and overall area under curve) was produced in Axium MicroFx coil specimens compared to the control. Reproduced with permission.[106] Copyright 2014, Elsevier B.V.

3. Shape Memory Polymers (SMPs)

As an intelligent material, SMP absorbs energy to overcome internal stress, can respond to external stimuli (solution, light, electricity, water, etc.), and has good features such as shape memory, biocompatibility, and deformability.[123] Biomedical devices manufactured employing SMPs could be implanted into the body in compressed form and then expanded to programmed form as needed. Because shape recovery could be facilitated by specific triggering mechanisms like temperature rise, the release of medical devices could be completed via micro-catheter instead of additional complex surgical operations.[2] Actuation mechanism selection for shape recovery is a key criterion in the fabrication of endovascular devices.[22] Currently, most biocompatible SMPs employed in medical applications are thermally activated. As heated higher than glass transition temperature (T_g), amorphous segments of SMP transition from glassy to rubbery state, permitting the polymer to deform with external load. After cooling lower than T_g and subsequent load release, a temporary shape is achieved. When the polymer temperature rises again above T_g, the polymer could return to programmed form autonomously without external stimuli.[2] For thermally actuated SMPs, increasing the polymer temperature above T_g causes the decrement in elastic modulus from glassy (≈10^9 Pa) to elastomer (≈10^6 to 10^7 Pa). In SMP foam, the decrease in modulus corresponds to expansion force during thermal actuation (< 1 kPa at recovered strain over 50%) that is less[124,125] than the force (700 to 5000 kPa) needed to rupture aneurysm wall.[126] After cooling, the original modulus is almost completely recovered and the first shape is stabilized. As SMP T_g is higher than body temperature (37 °C), an external heating mechanism like electrical (resistive) or photothermal (laser) is needed.[127] Compared with conventional materials, SMP has several advantages such as adjustable T_g, biodegradability, large deformation, lightweight, and low cost.[123,128–131] Because of shape memory influence, medical devices dependent on SMP could be implanted in the body in contracted or folded state through minimally invasive surgery and recovered to the required original shape at the aimed position. The most positive feature of SMP is that its stiffness is tunable.[123] SMP has two phases, fixed and reversible, having inseparable synergy to retain its original form and contribute to its capability to shape-shifting. The fixed phase plays an important task in keeping and recovering the initial shape and preventing material flow deformation. Fixed phase possesses

Table 2. Methodology and clinical outcomes with polymeric materials for intracranial aneurysm treatment.

Material	Methodology	Clinical outcome	Reference(s)
Bioactive polymer-platinum coils	Platinum coils having bioactive PGLA/poly(D-L-lactic-co-glycolic acid) (PLGA) or PGA embedded in coil or coated were delivered endovascularly into aneurysm and detached to cause embolization. Biodegradable polymer was developed to enhance tissue response and fast formation of thrombus.	Aneurysm healing enhanced compared to bare platinum coils, but declared recurrences ranged from 15–37% of patients.	[113, 117, 118]
Hydrogel-coated coils	Hydrogel-coated platinum coils were delivered endovascularly into aneurysm and detached to cause embolization. Blood contact caused swelling of hydrogel, rising aneurysm completing.	Aneurysm volumetric occlusion enhanced compared to bare platinum coil with recanalization forming in 22–28% of patients.	[119, 120]
Liquid embolics	Polymer suspended in solvent was injected into aneurysm by balloon catheter blocking aneurysm neck, and polymer precipitated and solidified within aneurysm. It was frequently utilized in connection with stenting.	High volumetric occlusion of aneurysm was obtained, however process was more complex. Recurrence was demonstrated in 5–13% aneurysms.	[121, 122]

greater crystalline melting temperature or T_g. But the reversible phase has lower melting temperature or T_g. At the reversible phase, SMP can undergo reversible hardening and softening alters with changing external conditions (e.g., temperature) that promote polymer deformability.[123] GDC-based coils are developed to remain in the body, therefore it is crucial that SMPs utilized for endovascular embolization do not relax over time, causing the aneurysm to recur.[2] SMP in the form of an aneurysm can completely fill the site and block blood flow.[18]

Endovascular devices could be enhanced by SMP coating that fills spaces between coils (**Figure 10**). Another approach is the production of a coil-free foam device that uses a patient-specific shape to occlude aneurysm after its form has been recovered (Figure 10).[22] SMP is crimped over a platinum-tungsten coil for catheter delivery and self-expands to a predefined volume upon contact with blood (**Figure 11**).[132] TrelliX coil is coated by polyurethane (PU) SMP foam, allowing the device to fill 2.5 times more volume than GDCs after activation. Foam expansion could be triggered after aneurysm coiling, supposed to raise packing density and prevent recurrence. It was reported that the polymer formulation of this device promoted healing through neoendothelium formation and promoted collagen deposition on the material surface.[133–135] Also, it was reported that these devices had an acceptable occlusion rate for the in vivo rabbit model where progressive occlusion was seen.[134] PU SMPs were implemented as a coating on platinum coil in the modified adaptation of coil embolization, showing hopeful outcomes with in vitro experiments and in vivo animal works.[136,137] But, even by SMP-enhanced coil, coil compaction risk, and recanalization available technical and clinical drawbacks because of the resorption of polymer coating.[123,138]

Bioactive coils depended on SMP have been designed to replace metal coils. As in contact with blood, the polymer-coated platinum coil swells. Finally, the coil can expand up to ninefold from its initial state. Therefore, the technology could maximize coil volume while reducing the number of coils needed and decreasing the treatment time.[40] Compared to a metal coil, a hybrid-hydrogel coil performs better for causing aneurysm occlusion, and this was confirmed by animal experiments.[139] In the porcine aneurysm model, SMP caused a higher decrement for aneurysm cross-sectional area in comparison to metal coil.[133] In the rabbit elastase model, an aneurysm treated by the SMP coil possessed more connective tissue and less debris than those treated by the metal coil at 180 days after embolization.[135] It was found that SMP coils were efficient and safe for the treatment of intracranial aneurysms over 12 months in human studies.[132]

Kunkel et al.[2] characterized aliphatic urethane-based SMP for determining efficiency as a new material in embolization. The time of shape recovery was lower than 11 s with SMP formulations, being low enough to change shape during the embolization procedure.[2] In the context of an implantable embolic device, SMP should have T_g higher than body temperature (37 °C) but lower than tissue damage threshold (45 °C).[140] If T_g is higher than body temperature, the implant exists in a continuously malleable state and does not have a definite shape; however, at temperatures above 45 °C, body tissues may begin to be damaged. Some candidate formulations were identified that have T_g higher than body temperature and lower than the threshold to cause

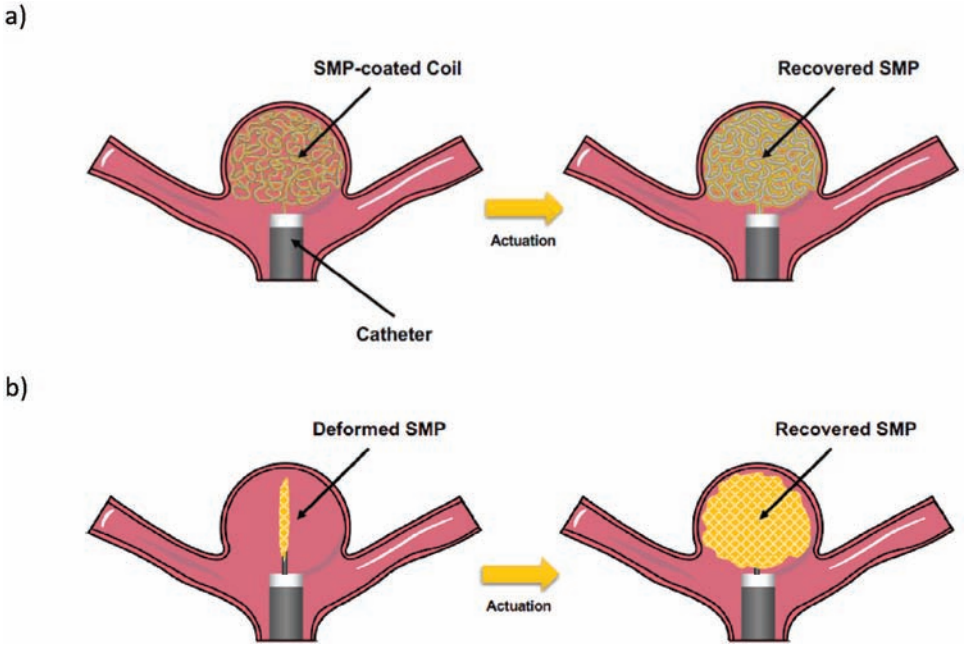

Figure 10. Schematic view for two approaches to manufacture SMP-based endovascular devices in intracranial aneurysm therapy. a) SMP-coated coils. Reproduced under the terms of the CC BY 4.0 license.[22] Copyright 2022, The Authors. b) SMP coil-free foams. Reproduced under the terms of the CC BY 4.0 license.[22] Copyright 2022, The Authors.

tissue damage. Researchers showed low-stress relaxation and high-strength behavior, suggesting that they could potentially be applied to endovascular embolization in intracranial aneurysms.[2]

SMP foam is a favorable biomaterial in endovascular embolization applications owing to shape recovery ability and porosity. SMP foam is more efficient than embolic coil at causing flow stagnation in the treated aneurysm.[141] The embolization device composed of an SMP foam-on-wire device and an optional laser-heated saline-injected cable tube delivery and detachment device for SMP foam expansion is illustrated in **Figure 12**.[137] Recently, PU-based SMP foam has been studied as a material to occlude aneurysms with hopeful output[142] and biocompatibility.[142,143] Metcalfe et al.[142] presented a number of experimental and animal studies employing PU SMP foam for the therapy of carotid aneurysms. After compaction, SMP foam was implanted into the aneurysm and could gently fill the aneurysm during expansion because of the shape memory effect. This technique could obviously reduce operation complexity and avoid coil-induced rupture. After three weeks, angiographic scores were enhanced with SMP. Histological outcomes indicated that foam had a thick layer of neointima on its surface; most of the aneurysm neck was sealed with connective tissue and thrombus. Researchers stated that because of T_g was 60 °C, SMP foam did not fully deploy at body temperature. So, it only sealed most of the aneurysm neck. It will have a better influence if T_g is lowered to near body temperature.[142] Metcalfe et al.[142] demonstrated that foam pore size could affect cellular infiltration and stable tissue

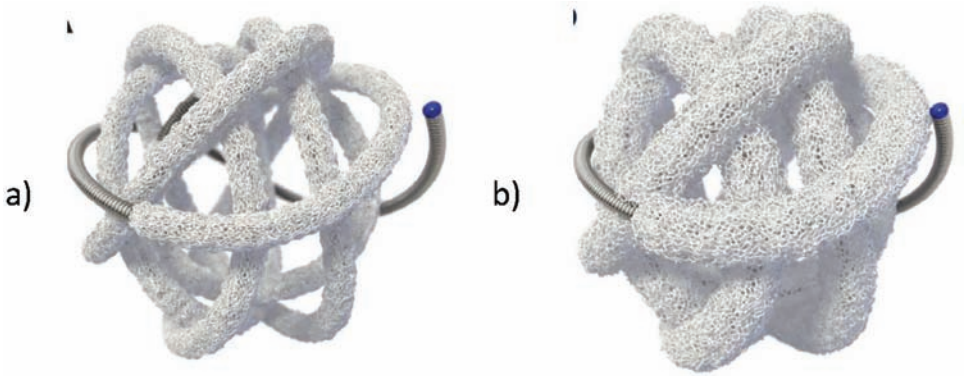

Figure 11. SMP coil at a) crimped and b) expanded shapes. Polymer expands when it meets blood. Pores for expanded shape are ≈200 μm diameter and promote thrombus creation. The volume occupied by a fully expanded polymer coil is about four times greater than the volume occupied by a crimped form. Reproduced under the terms of the CC BY-NC license.[132] Copyright 2023, The Authors.

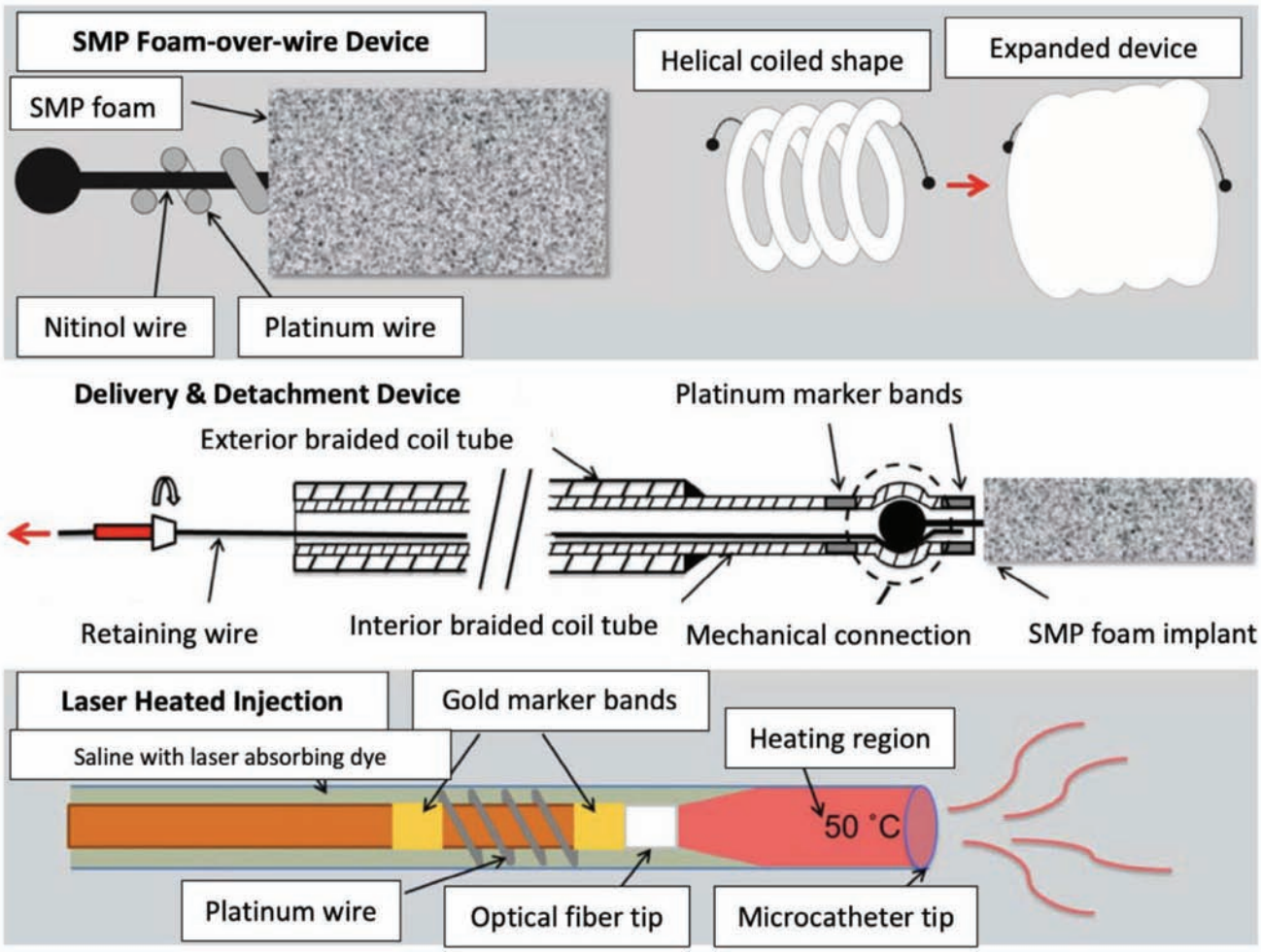

Figure 12. Schematic views of SMP foam-over-wire (top), delivery and detachment device (middle), and laser mechanism for heating (bottom). Reproduced with permission.[137] Copyright 2015, Wiley Periodicals, Inc.

integration in foam. Foam having about 250–800 μm pore diameter was found to be effective in occlusion of porcine sidewall aneurysm and served as a good scaffold for connective tissue deposition, providing positive long-term healing.[15] The pore size of SMP foam could be tailored with changing initial monomer concentrations during synthesis,[144] allowing optimization of cellular infiltration, proliferation, and retention.[99] Maitland et al.[126] presented the development and laser deployment of the SMP foam device. Results from the in vitro basilar aneurysm model without and with flow demonstrated successful therapy, with flow rate influencing foam expansion and temperature at the aneurysmal wall. Zero flow caused rapid, full expansion with overheating at the aneurysmal wall. Low (diastolic) flow caused slow, full expansion with minimum temperature increment at the aneurysmal wall. High (systolic) flow caused incomplete expansion.[126] PU SMP foams were utilized to create uniform embolization plugs (**Figure 13a**), which showed stable thrombus and complete aneurysm neck endothelialization in 90 days (Figure 13b).[136] SMP foam in porcine saccular aneurysm models has been declared to have rose angiographic occlusion, improved healing marked with mature connective tissue, and a thicker neointima layer in comparison with the metal coil.[133,136] Although both hydrogels and SMP foams demonstrate volume-filling ability, SMP foams show interconnected pores hundreds of microns in diameter in comparison with hydrogel pore sizes lower than 10 μm.[144,145] The SMP foam interconnected porosity behaves as a scaffold for blood flow, thrombus formation, and tissue healing through material volume.[133,136] Ultra low-density PU SMP was used to support vessel and aneurysm embolization.[144,146] Material could be crimped for catheter delivery and self-expands to a predefined volume as a porous structure within the vessel (warm aqueous conditions). Expanded form possesses great surface area and promotes the formation of thrombus throughout its structure.[132] J. Wang et al.[138] developed a biocompatible and highly porous PU SMP material for the fabrication of endovascular devices in the treatment of complex intracranial aneurysms. These researchers claimed that porous PU SMP material and electrical resistance heating trigger mechanism can enhance long-term therapeutic outputs of endovascular intracranial aneurysm therapy.[138]

Foam-coated coil prior to and after compression is depicted in **Figure 14a**. Deployment of the device into an in vitro

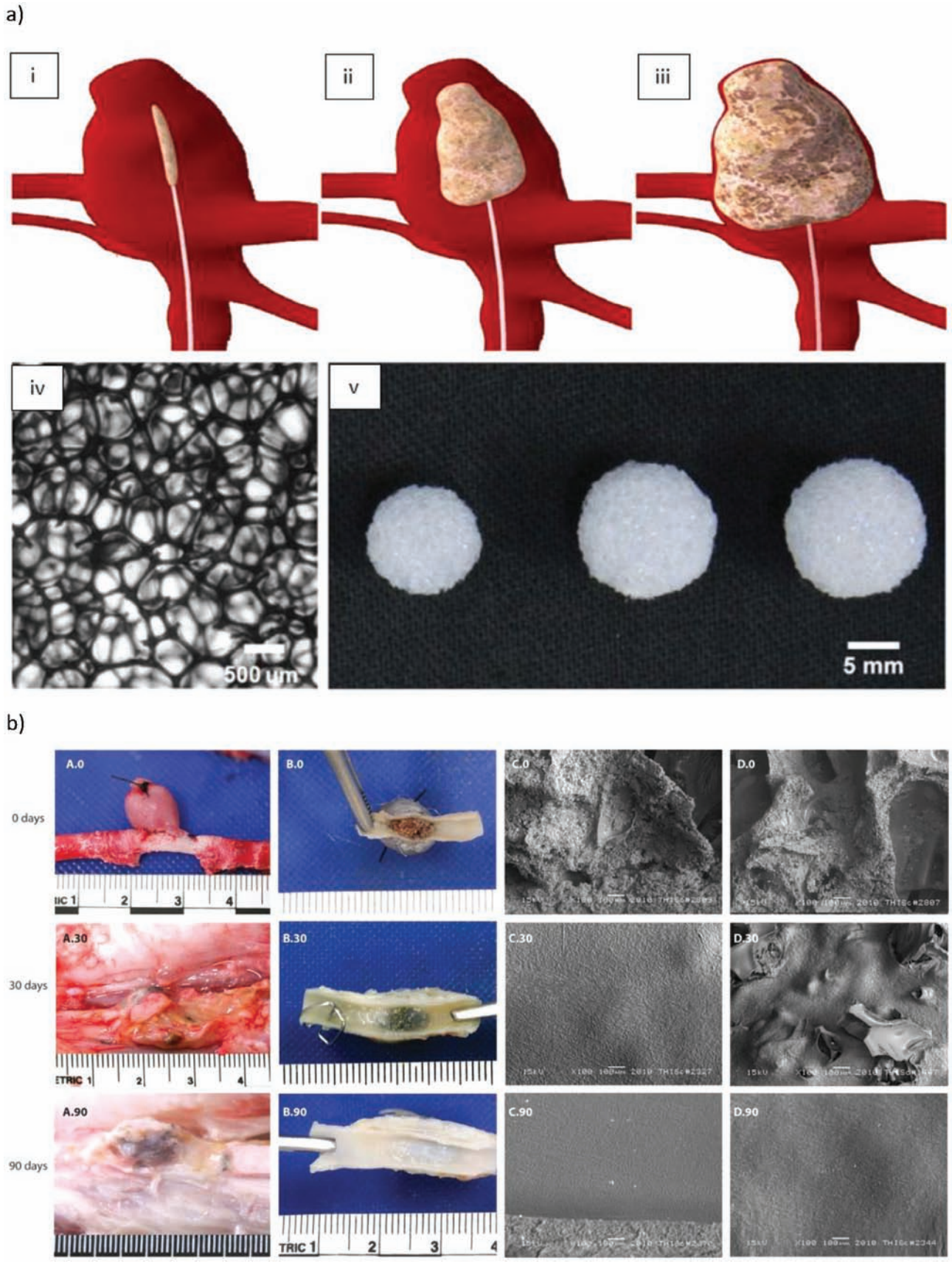

wide-neck aneurysm model is demonstrated in Figure 14b.[44] Both in vivo and in vitro observations demonstrated that SMP foam-coated embolization coils gave improved healing responses at the aneurysm site while maintaining pro-healing macrophage phenotype compared to bare platinum coils.[147]

In clinical medicine, therapy of wide-neck aneurysm will be different. It always requires staged treatment techniques, including stent-assisted coil embolization during the curing process. The technologies have been successfully proven in wide-neck aneurysms but fall short in the therapy of fusiform aneurysms with clearly identifiable necks.[123] Small et al.[148] presented prototype device for fusiform aneurysm treatment depended on thermally activated SMP. Two components of the device were the SMP scaffold and SMP embolic foam. The light-diffusing fiber was compressed into the device for photo-thermal activation. Functionality was studied with an in vitro model: Aneurysm lumen was successfully completed with foam, while the shape memory scaffold kept a flow channel.[148]

SMPs employed in endovascular embolization procedures are summarized in **Table 3**.

4. Polymer Blends

The use of polymers is widely attractive in endovascular embolization applications. However, polymers generally do not encompass all desirable properties such as aneurysmal recanalization, cytocompatibility, degradability, and long-term safety. Developing and synthesizing an entirely novel polymer could be a long and expensive procedure.[149] To overcome shortcomings when employing a single polymer in endovascular embolization applications, concepts of polymer composites or polymer blending have been employed. A polymer blend is composed of two or more polymers/copolymers mixed by physical technique to form a homogeneous mixture, developing novel material with combined features of original polymers (**Figure 15**). The physical properties of polymer blends can be changed, depending on the ratio of each polymer.

In the 2000s, polyglycolic and polylactide acids were added to coil lattice to cause inflammatory reactions, in the hope that recurrence and retreatment rates could be decreased. Results demonstrated that polymer was absorbed over several weeks period, showing thicker, denser neointimal tissue along the experimental aneurysm neck. Longer-term clinical trials are needed to show effectiveness, and prospective, larger, randomized trials are now being carried out to evaluate the long-term effectiveness of PGLA-coated coils and the capability to increase long-term neck and aneurysm healing by reducing the incidence of recurrence in the long term.[11] Polymer-coated coil might be safe for patients with aneurysm.[150] Matrix and Matrix2 are composed of platinum coil core by coating of PLGA. High recanalization rates were reported for Matrix coil compared to bare platinum coil.[151] Designed to mitigate issues with first-generation coils, Matrix2 coils improved over Matrix coils 8 months after treatment, but demonstrated important recanalization at long-term follow-up, about 18 months, which raised durability concerns.[114] Nexus and Axium are composed of platinum coil by PLGA and PLGA/nylon fibers intertwined in coil, respectively.[152,153] Short-term effectiveness and long-term safety for thin platinum coil coated by bioabsorbable polyglycolic acid (90%)/polylactide (10%) polymer were evaluated. Platinum coil coated by polyglycolic acid/lactide polymer may prevent recanalization after endovascular therapy of aneurysm.[154] It was declared that polyglycolide (90%)/polylactide (10%)-coated platinum coil speeded up clot fibrosis and decreased recanalization rate and aneurysm volume.[150] Skolarus et al.[155] presented two patients having mild clinical symptoms, who faced postprocedure neurological symptoms with white matter alternations on brain imaging after basilar tip aneurysm therapy by PGLA coil. Researchers hypothesized that symptoms and MR imaging findings of patients not all within the territory provided with the coiled vessel were because of the overexuberant inflammatory response associated with the PGLA coil.[155] For intracranial aneurysms, PGLA-coated coil embolization was not found to be superior to platinum coil in terms of aneurysmal recanalization.[156] PGLA-coated coils did not provide a better long-term ($\geq$ 12 months) recanalization rate than platinum coils in aneurysms treatment.[118] However, Hwang and Kim[157] declared that bioactive PGLA-coated coils were found to be a safe method for recanalization in patients with intracranial aneurysms.

Besides coated coil techniques, other coils were developed by biopolymers like PGLA in coil structure to retain acute full occlusion rate leading to biological reaction from foreign polymer.[11] Murayama et al.[158] evaluated bioabsorbable lactide/glycolic acid copolymer PLGA ribbons at the concentrations of 85/15, 75/25, 65/35, and 50/50 (**Figure 16**), which may promote cellular reaction in aneurysms, with animal study.

Figure 13. a) Recommended SMP foam device in aneurysm filling. i) Crimped (temporary form) device, delivered via catheter into aneurysm. ii) Intermediate view for expanded foam in aneurysm when it returns to permanent form with stimuli. iii) Treated aneurysm by fully expanded foam. iv) Foam detail. v) Foam devices. Reproduced with permission.[136] Copyright 2013, Wiley Periodicals, Inc. b) Gross and microscopic assessment of healing for implanted SMP foam. A.0) 30 min SMP foam implant in vein pouch model. B.0) En face view for aneurysm artery interface after 30 min in vivo. C.0) LV-SEM indicates partial protrusion of foam material in the lumen. D.0) Porous surface in contact with vessel lumen possesses patchy aggregates of fibrin-enmeshed erythrocytes attached to foam struts. A.30) Dissected aneurysm in situ after 30 days of implantation. Aneurysm outer surface consisted of dense white to slightly opaque connective tissue with patchy tan to golden brown discoloration. B.30) Excised aneurysm by two clips marking the cranial end. In patchy areas, this outer capsule was adherent to adjacent skeletal muscle. The left carotid artery was bisected parallel to the long axis to visualize the ostium of the left aneurysm sac. The cranial end was labeled by two clips. C.30) Most of the ostium demonstrates imprint for polymer foam under endothelial covering. D.30) 30 days after implantation, a focal area of disruption is present and the polymer is subjected to lumen. A.90) Right carotid in situ indicated outer surface of artery and aneurysm with multifocal adhesions of dense white connective tissue. B.90) The right carotid artery was bisected parallel with the long axis to visualize the ostium of the left aneurysm sac. The surface covering the ostium was white, glistening, and looked intact. C.90) A bisected section of the artery and an endothelial cell-covered surface are seen in the en face ostium of the aneurysm sac. D.90) No evidence of proliferating mural thrombosis. Endothelial cell morphology across the ostium is mostly spindle-shaped and parallel with the long axis. Reproduced with permission.[136] Copyright 2013, Wiley Periodicals, Inc.

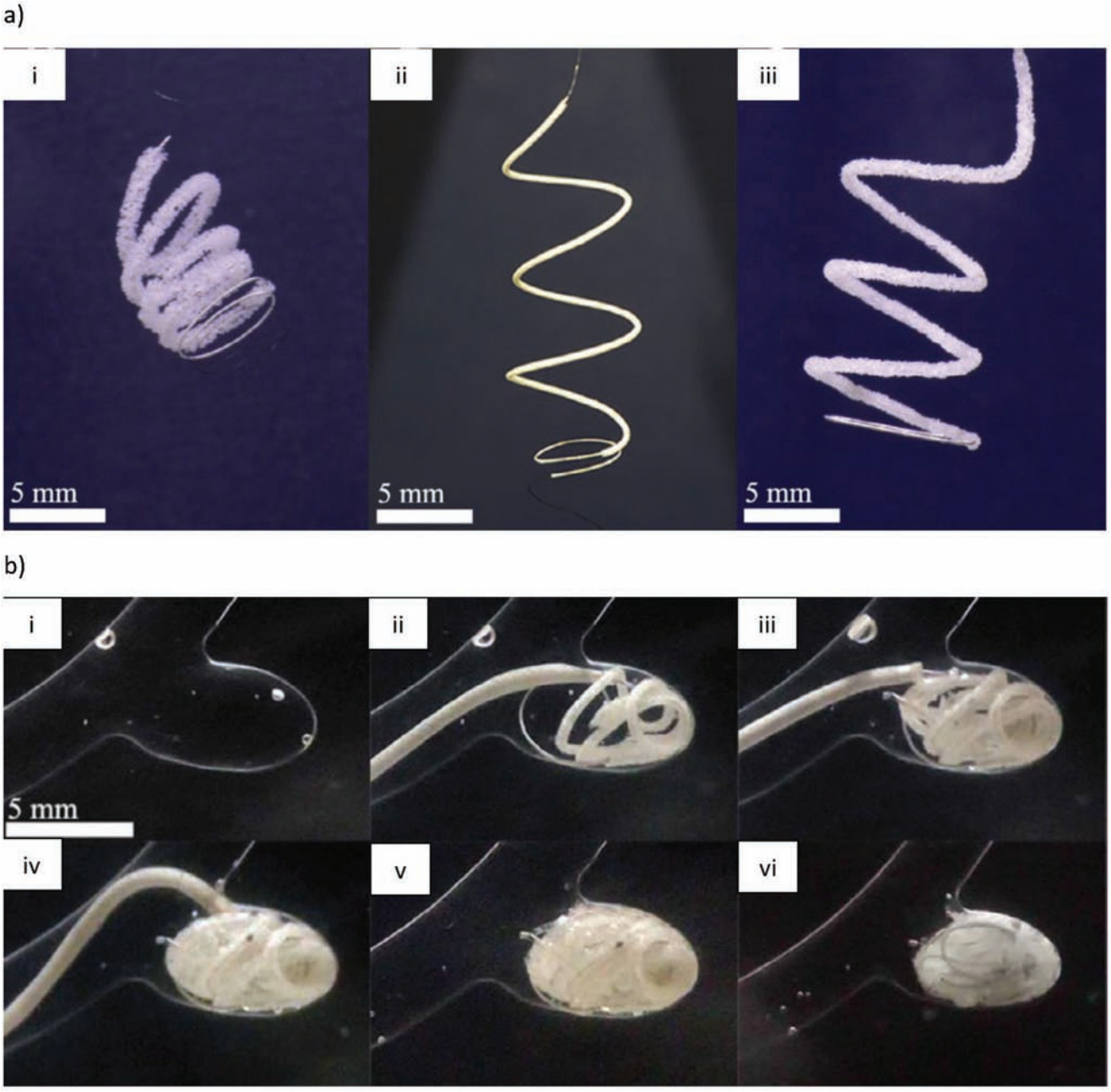

Figure 14. a) SMP foam-coated coil. i) Prior to radial compression. ii) After radial compression. iii) After expansion at 37 °C water at 30 min. Reproduced with permission.[44] Copyright 2017, IPEM. published by Elsevier Ltd. b) SMP foam-coated coil embolization device deployment in in vitro wide-necked aneurysm model. i) Aneurysm model before device deployment. Air bubbles are seen. ii) First device deployed. iii) Second device deployed. iv) Third device deployed. v) Packed aneurysm model 30 min after implant of the third device. vi) Reverse side of packed aneurysm model 30 min after implant of the third device. Reproduced with permission.[44] Copyright 2017, IPEM. Published by Elsevier Ltd.

Liquid embolics from poly(propylene glycol) diacrylate (PPODA) and pentaerythritol tetrakis (3-mer-captopropionate (QT),[159] poly(N-isopropylacrylamide-*co*-acrylic acid) (NIPAAM)[77] polymer systems were developed. Both polymer systems are non-adhesive and non-degradable and have been taken into consideration for usage in the treatment of intracranial aneurysms.[78,86] Usage of these polymers can prevent recanalization seen in coil embolization by obtaining higher filling volume in aneurysms. Also, these materials do not create toxic byproducts like *n*-BCA and/or utilize hazardous solvents like DMSO.[92]

Poly(NIPAAm-*co*-HEMA-acrylate)/poly(NIPAAm-*co*-cysteamine) blends, simultaneous physical and chemical gelling polymer system, can be utilized as a liquid-to-solid embolic agent with use in vivo endovascular embolization for intracranial aneurysm.[96] In vitro properties of crosslinking

Table 3. SMPs used for aneurysm occlusion in the literature.

SMP	Form	Characteristics	Highlighted results	Reference(s)
PU	Cold hibernated elastic memory (CHEM) foam	* Biocompatible * Non-mutagenic * Non-toxic * Self-deployable	* Cellular invasion and reendothelialization. * Minimal inflammatory reaction. * Successful occlusion of carotid aneurysm.	[142]
Hexamethylene diisocyanate (HDI), N, N, N', N'-tetrakis(2-hydroxypropyl) ethylenediamine (HPED), and triethanolamine (TEA)	Foam	* Laser-activated	* Applicability showed in vitro basilar aneurysm model. * Full expansion in absence of flow.	[126]
HDI, HPED, and TEA	Foam-augmented stent	* Laser-activated	* Applicability in embolization for non-necked fusiform and wide-necked aneurysms.	[148]
PU	Foam	* Heat-actuated * Biocompatible	* Aneurysm healing through increased collagen deposition on the material surface. * SMP caused larger decrement in aneurysm cross-sectional area in comparison to bare metal coil.	[133]
Trimethyl-1,6-hexamethylene diisocyanate (TMHDI), HPED, and TEA	Foam	* Biocompatible * Cytocompatible	* Applicability of intracranial saccular aneurysms. * Excellent packing volume. * Scaffolding capability.	[44]
TrelliX (Shape Memory Medical Santa Clara, California, USA)	Foam	* Temperature activated * First report about clinical experience with SMP coil in intracranial aneurysm embolization	* Greater packing density. * Porous polymer scaffold promotes thrombus formation.	[132]

polymer systems (PPODA and QT) with two different liquid contrast agents (Conray and Omnipaque) for cerebral aneurysm embolization were determined. PPODA-QT was evaluated for feasibility of delivering by mock delivery to the model aneurysm. Swelling, cytotoxicity, and compression testing were performed. Conray-formulated gels gave smaller initial cytotoxicity whereas they responded to higher swelling and faster degradation. Conray-formulated gels might be better equipped to promote neointimal tissue growth in vivo, helping to minimize concerns about excessive swelling and degradation.[88] PPODA and QT monomers are liquid at room temperature, however, when combined with nucleophilic activators in aqueous media they react chemically by Michael-type addition to create hydrogel.[86,87] The concept was validated in vivo by employing a canine model by creating an aneurysm in the lateral wall of the carotid artery.[89] PPODA and QT were blended in 2:1 mole to form a hydrophobic monomer solution. Before administration, the monomer solution was blended at a 3:1 ratio with Conray, ionic contrast dye, at 11.0 pH for 2 min.[87,88] Incorporation of great pH contrast initiates polymerization while giving a mechanism to monitor administration for embolic. PPODA-QT possessed 10 min gel time, but time could be decreased by manipulating the PPODA/QT ratio, tuning pH, and rising blending time of monomer and initiating solutions.[86,88] The toxicity of the activating solution is a disadvantage of the system. Conray is cytotoxic, especially at high pH, but co-administration with polymeric matrix partially improves toxicity.[88] This work demonstrated that the application of polymers is suitable for usage in aneurysms, however small specimens number and lack of control prevented the comparison of efficiency with other polymer embolics.[92] Liquid-to-solid gel polymer (poly(ethylene glycol) diacrylate-QT (PEGDA-QT)) may fill aneurysm more completely than existing embolization materials, decreasing aneurysm recurrence. PEGDA-QT gels were developed employing various molecular weights PEGDA and their properties (crosslink integrity, cytotoxicity, gel time, mass change, protein release capability) were investigated in vitro. Although molecular weight 700 PEGDA-QT swells more and degrades more rapidly than molecular weight 575 PEGDA-QT, the protein release properties and cytocompatibility might prove to be more advantageous for aneurysm therapy in vivo.[160]

NIPAAM polymers exhibit less critical solution temperature (32 °C) in aqueous media, below which dissolve and above which precipitate out of solution.[74] This permits the polymer to be delivered in liquid and then entropically removed from solution after injection to create solid hydrogel. NIPAAM-based polymers were functionalized to form degradable[84] and radiopaque embolic versions.[85] An important novelty was the copolymerization of NIPAAM with other polymers to form a liquid-solid transition platform in which chemical and physical gelation takes place simultaneously under physiological conditions.[81,82] Dual gelation systems combined

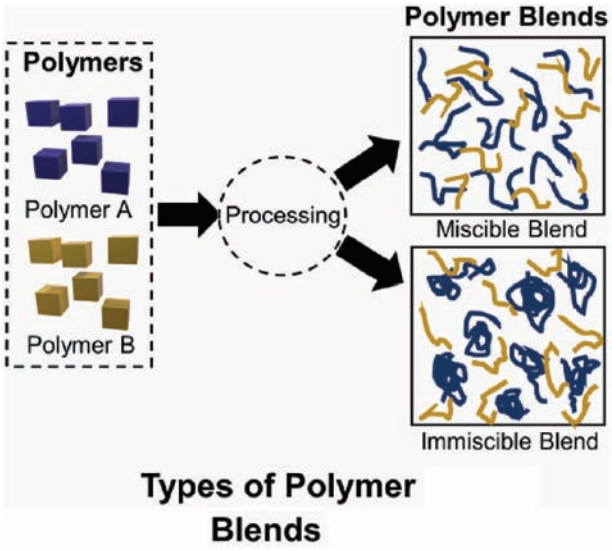

Figure 15. Schematic representation of polymer blends. Homogeneous (miscible) blends are single-phased with one T_g. Heterogeneous (immiscible) blends have phase separation and show two or more T_gs. Reproduced with permission.[149] Copyright 2021, Elsevier Ltd.

NIPAAM-co-cysteamine (NC) polymers containing thiol and either NIPAAM-co-hydroxyethimethacrylate-acrylate (NCHA) or NIPAAM-co-cysteamine-vinylsulfone (NCVS) polymers, both containing vinyl groups. NC-NCHA or NC-NCVS blends include thiol and vinyl groups that undergo Michael-type addition at pH 7.4 to chemically crosslink polymers in body temperature.[161] In the in vitro model, dual gel exhibited adhesive features and was loosely adhered to the catheter; this is not beneficial for clinical use because of the potential for delivery system entrapment.[82] Live/dead staining and cell proliferation works with T3T mouse fibroblasts demonstrated that both systems had great biocompatibility.[82,162] As proof-of-concept work, a swine model via surgically created aneurysm was successfully treated by NC-NCHA. Work confirmed the system's capability to be delivered with a catheter and solidified in the aneurysm at physiological conditions.[82] But aneurysm recanalization was seen shortly after the process.[92]

Some polymer blends employed in endovascular embolization procedures are summarized in **Table 4**.

5. Polymer Composites

A polymer composite is a material that has at least two physically combined phases (continuous and dispersed [or discontinuous] one embedded in continuous phase). The continuous phase behaves as a "matrix", whereas the discontinuous phase behaves as "reinforcement" (**Figure 17**).

It is important that the endovascular device needs to be visible by X-ray fluoroscopy in order for medical doctors to pinpoint orientation and location during deployment. Polymeric materials are invisible to radiographic imaging methods and thus radiopaque additives must be added to polymer for their usage in endovascular embolization applications.[2] Radiopaque polymers in which the radiopacifying derivative is covalently bonded to

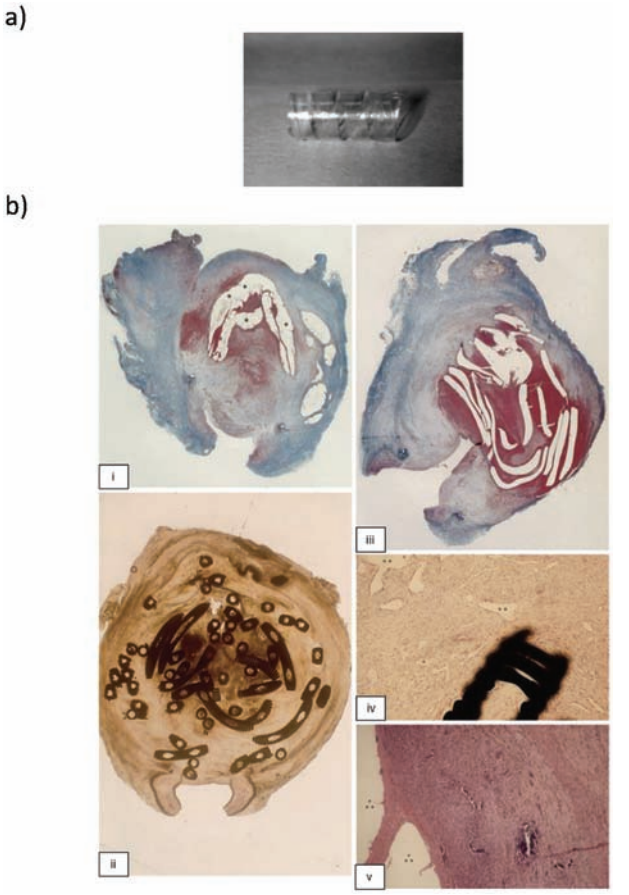

Figure 16. a) Spiral-shaped bioabsorbable polymeric ribbon (Diameter = 5 mm, length = 8 mm). Reproduced with permission.[158] Copyright 2002, American Heart Association, Inc. b–i) Low-magnification light microscopy for aneurysm treated via 50/50 PLGA 14 days after embolization (Masson trichrome; magnification ×3.1). Note highly organized connective tissue along the neck of the aneurysm through small polymer content (star mark) in the sac. There is an intraaneurysmal unorganized clot near the sac. ii) Low-magnification light microscopy for aneurysm treated via GDCs 14 days after embolization (hematoxylin and eosin; magnification ×3.1). In the center of the sac is the intra-aneurysmal unorganized clot. iii) Low-magnification light microscopy for aneurysm treated via 85/15 PLGA 14 days after embolization (Masson trichrome; magnification ×3.1). Note neck remnant and the existence of intraaneurysmal unorganized clot in the sac. iv) High-magnification light microscopy for an aneurysm treated with GDC 14 days after embolization. Soft connective tissue surrounds coils, and there are lightly organized collagen and fibroblasts. Note multiple microneovascular formations (star mark) (hematoxylin and eosin; magnification ×25). v) High-magnification light microscopy for aneurysm embolized with 50/50 PLGA 14 days after embolization. There is a moderate inflammatory reaction consisting primarily of foreign body giant cells and macrophages (arrows) (hematoxylin and eosin; magnification ×25). Star marks denote polymer. Reproduced with permission.[158] Copyright 2002, American Heart Association, Inc.

the polymer backbone will create homogeneous, non-leachable materials that develop mechanical characteristics substantially equivalent to those of the main polymer.[163] Radiopaque embolics can be trackable in vivo. Onyx liquid embolic agent is non-adhesive, biocompatible including ethylene-vinyl alcohol (EVOH) copolymer with DMSO incorporated into tantalum

Table 4. Some polymer blends employed in endovascular embolization.

Polymer blend	Form	Characteristics	Highlighted results	Reference(s)
PPODA and QT	Gel	* Radiopaque	* Easily deliverable. * Experiments represented more difficult situations than available in vivo, and thus the declared conclusions are likely an overestimation of in vivo conclusions. * Initial cytotoxicity might be more significant than long-term parameters when selecting optimum formulation in aneurysm embolization.	[88]
Poly(NIPAAm-*co*-HEMA-acrylate)/poly(NIPAAm-*co*-cysteamine)	Gel	* Biocompatible * Physical and chemical gelling * Waterborne	* Delivered endovasculary and injected into aneurysm sac. * By optimizing injection volume and gelation features, nearly complete occlusion can be obtained.	[96]

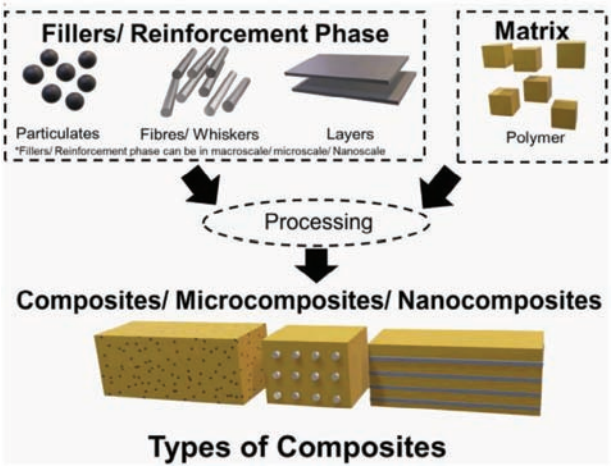

Figure 17. Schematic representation of polymer composites. Reinforcement is combined with a polymeric matrix to create a composite. Reproduced with permission.[149] Copyright 2021, Elsevier Ltd.

powder and this combination makes Onyx radiopaque.[11] When in contact with liquids, DMSO rapidly separates phase from copolymer and forms in situ solidification, allowing embolic material to be delivered at the aneurysm lumen.[22] Onyx's high density gives a 20% polymer concentration ideal for aneurysm embolization. The high complication rate is appreciated with low molecular weight Onyx, having a great incidence of reflux in the parent artery and distal migration of Onyx to distal unrelated arterial territories, causing strokes. Besides, the micro-catheter used with Onyx must be removed slowly due to the risk of arterial tear, aneurysm rupture, massive intracranial hemorrhage, and death.[11]

Trufill(Codman Neurovascular, Raynham, MA) was the first FDA-approved liquid polymer embolic in the treatment of intracranial saccular aneurysms.[164] It is composed of *n*-BCA liquid polymer, ethiodized oil, injectable radiopaque diagnostic agent, and tantalum. Liquid materials are injected by micro-catheter and solidified upon contact with ions available in the blood. Solidification time is controlled by tuning the proportion of ethiodized oil into a liquid polymer blend. Complications from the use of cyanoacrylate like *n*-BCA are acute and chronic inflammatory reactions that may take place in vessel walls or surrounding tissue and recanalization.[165]

Radiopaque bismuth (III) oxide was incorporated into the solution possessing suitable precipitation properties and angiographic assessment, for the in vitro aneurysm model. Cellulose acetate, poly(acrylonitrile), poly(butyl methacrylate), poly(ethyl acrylate-*co*-methyl methacrylate), poly(ethyl methacrylate), poly(methyl methacrylate), poly(vinyl acetate), poly(vinyl butyral), poly(vinyl chloride), and poly(vinyl formal) were selected as polymers. For solvents, diethylene glycol dimethyl ether, dimethyl isosorbide, dimethyl sulfoxide, ethanol, ethyl lactate, DL-α,β,-isopropylidene-glycerol, glycerol formal, glycofurol, *N*-methyl 2-pyrrolidone, 1,2-dimethoxyethane, tetrahydrofurfuryl alcohol, and water were used. Precipitation of each solution was evaluated in PBS of pH 7.4 at 37 °C to mimic the physiological case. 1,2-dimethoxyethane solutions of methacrylates having great molecular weight such as poly(ethyl acrylate-*co*-methyl methacrylate) or poly(methyl methacrylate) were satisfactory as embolic polymers. Because of great solubilizing capacity and adequate viscosity, *N*-methyl 2-pyrrolidone was the solvent for selected preformed polymers. Highly viscous poly(ethyl acrylate-*co*-methyl methacrylate) and cellulose acetate solutions were not feasible as embolic liquids in the in vitro model.[67]

Cellulose (microcrystalline and powder) and partially substituted cellulose acetate (two viscosity values) were chosen for beginning materials to develop iodine-including polymer composites. Embolic liquids were tested for precipitation characteristics at PBS (pH 7.4) that mimic physiological conditions employing an in vitro model. A sheep model was utilized for evaluating in vivo radiopacity and precipitation characteristics of a greatly concentrated solution of cellulose acetate 2,3,4-triiodobenzoate mixed ester. Cellulose acetate iodobenzoate mixed esters

dissolved in dimethyl isosorbide or diglyme can be feasible embolic fluids in aneurysm therapy.[163] Dudeck et al.[91] evaluated iodine-containing PVA dissolved in small angiotoxic organic solvent NMP during embolization of porcine wide-neck aneurysm. Fourteen carotid sidewall aneurysms were created in seven swine. Liquid embolic was well seen by fluoroscopy and exhibited a good precipitation pattern that allowed controlled polymer delivery. Ten aneurysms (71%) were initially entirely occluded, while minimal polymer leakage was seen in 1 aneurysm. The other four aneurysms (29%) were nearly entirely occluded. An animal presented fatal rebleeding from anastomosis after uneventful embolization. Aneurysm embolized by iodine-containing PVA was well differentiated from the parent artery without beam-hardening artifacts in multisection CT angiography and no susceptibility artifact was detected on MR imaging. Histological observation showed that all aneurysms were covered by the membrane of fibroblasts and endothelial cell layer, and a good intraaneurysmal inflammatory response to polymer was seen. Therefore, iodine-containing PVA dissolved in NMP was effective for the embolization of wide-necked aneurysm.[91]

The performance of three detachable hydrogel filament compositions (polyethylene glycol opacified by aromatic iodine, polyethylene glycol opacified by barium sulfate, or polypropylene glycol opacified by barium sulfate) in rabbit experimental aneurysms was compared. Embolization of experimental aneurysm by hydrogel filament caused durable histological and angiographic occlusion from 2 and 26 weeks.[51] To replace the metallic embolization coil with polymer, PVA hydrogels were prepared as bilayers. The hydrogel layer was fabricated by blending aqueous PVA solution with tantalum particulates for radiopacity, crosslinking the mixture with a glutaraldehyde crosslinking agent, and casting it into an aimed thickness film. It was found that the linear expansion and swelling ratio of hydrogel film can be controlled with crosslinking density. The time needed to reach the equilibrium swelling state was 2 min. Hydrogel film demonstrated sufficiently great elastic modulus appropriate for insertion to a catheter. Bilayer including 16.5 vol% tantalum was seen under X-ray having a Hounsfield unit (HU) value similar to human bone. In the occlusion test via glass aneurysm model, a high packing density of 66% was obtained, which was much greater than the platinum coil. The conclusion suggested that polymeric coil with less price and greater packing density can be an option to replace platinum coil as embolic material.[16]

Wei et al.[166] fabricated embolic microspheres by employing poly(carbonate urethane) (PCU) and iron oxide (Fe_3O_4) particles (0, 10, 15, and 20 wt%) (**Figure 18**a,b). Results indicated that composites can enhance cell proliferation and adhesion of vascular smooth muscle cells in vitro tests conducted in subcutaneous rat models, especially composites containing 10 and 15 wt% Fe_3O_4. Composites demonstrated smaller hemolysis ratios and showed higher clotting time, giving better hemocompatibility than PCU. Composite containing 15 wt% Fe_3O_4 was found to be the best option for promoting neointima formation to decrease recanalization and improve occlusion rate.[166]

The lack of radiopacity and bioinertness of SMP limit its potential applications in the interventional radiology technique.[18] The developed SMP foam aneurysm-filling device needs to meet some objectives. The first requirement is the opacification of SMP foam, permitting visualization during endovascular treatment employing standard imaging (fluoroscopy). The second need is that the mechanical characteristics of opacified foam should be similar or better in comparison with the original SMP foam. When SMP foam was doped with 4% tungsten particles, the second requirement was met by maintaining its integrity and increasing modulus. The third requirement concerns the chemical properties of the material. The fourth requirement is that developed material should not have a greater inflammatory response in vivo in comparison with FDA-approved materials. This was met with nearly complete healing of the aneurysm region after 90 days and the absence of inflammation in comparison with suture material.[15]

Hampikian et al.[3] used PU SMP and 3 wt% tantalum filler-based SMP composites as candidates for aneurysm coils (**Figure 19**a). Tantalum filler did not contribute to shape recovery response (Figure 19b), but increased modulus. Radiopaque SMP embolic coil increased the probability of occurring stable tissue matrix. It reduced aneurysm recanalization risk in comparison to platinum coil. Deploying of the SMP coil into the aneurysm is demonstrated in Figure 19c. Hot water employed for simulation had the same pressure and velocity as in vivo flow. A coil was implanted to model verticality status. When the coil was exposed to hot water, it recovered its initial state within the glass aneurysm. Outcomes showed that coil recovery was not hindered by hydrodynamic force. At the same time, the coil remained stable in the aneurysm dome without migrating to the cavity.[3] Wong et al.[167] developed polymer composites of PLGA containing bismuth (III) oxychloride (BO), barium sulfate ($BaSO_4$), and tantalum (Ta) and they are clearly visible in radiographic images while maintaining shape memory effect (**Figure 20**a). In vivo embolic plugs in the rabbit model indicated that the prototype was seen by fluoroscopy and complete occlusion formed in less than 2 min in all cases (Figure 20b).[167] It was reported that tungsten-doped PU-based SMP foam was a suitable filling material for intracranial aneurysm therapy.[15,168] Rodriguez et al.[15] determined the minimum content of tungsten necessary to make SMP foam visible under imaging methods and reported increasing radiopacity by adding tungsten filler, while keeping similar physical properties of SMP foams. It was declared that 4% loading of tungsten into SMP foams was an efficient method for enhancing radiopacity while conserving the chemical, physical, and mechanical properties of the original polymer.[15] J. Wang et al.[169] formed highly porous multi-walled carbon nanotube (CNT)/SMP nanocomposites in endovascular treatment of intracranial aneurysm (**Figure 21**a,b). Infiltration of CNTs into PU SMP foam was studied and Joule heating was shown for SMP shape recovery at endovascular treatment (Figure 21c). It was found that CNTs could successfully infiltrate SMP foam, giving adjustable resistivity and shape recovery time, and CNT infiltration decreased the T_g of SMP and changed its mechanical properties (**Figure 22**a–c). CNT infiltration of SMP foam is the hopeful procedure for the development of electrically triggered embolic devices in intracranial aneurysm therapy (Figure 22).[170] Hybrid nanocomposites of radiopaque fillers ($BaSO_4$ and hydroxyapatite [HaP]) in PU SMP matrix were developed via a twin-screw extruder and mechanical, radiopacity, shape recovery, and thermal characteristics of hybrid composites were compared to those of neat SMP and its composites with single filler. Shape recovery properties of hybrid nanocomposites were reduced by 20–30%

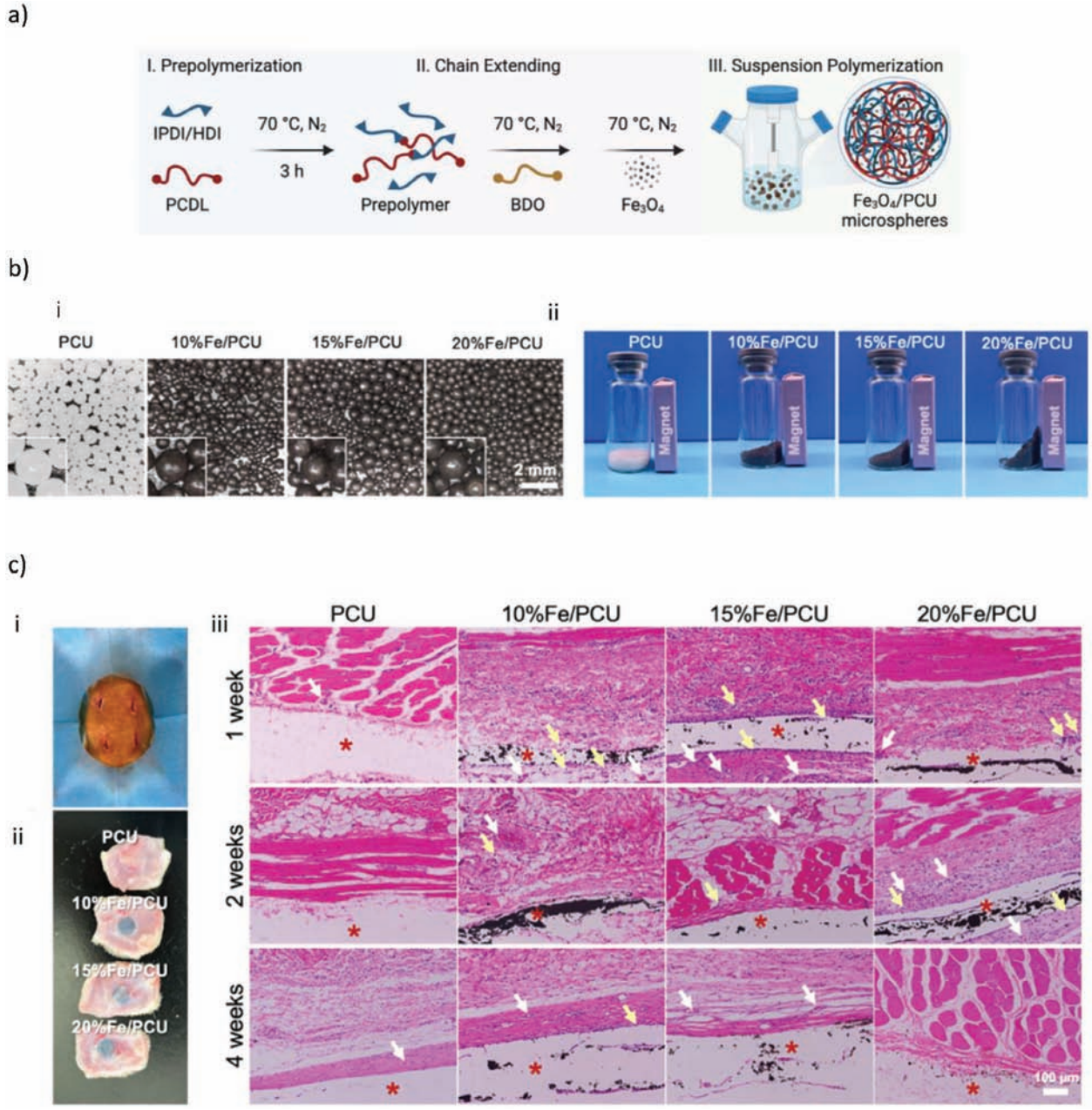

Figure 18. a) PCU and Fe_3O_4/PCU microspheres synthesis. After prepolymer formation, chain extender and Fe_3O_4 nanoparticles were incorporated to produce magnetic PCU microspheres containing Fe_3O_4. Reproduced with permission.[166] Copyright 2022, American Chemical Society. b–i) Microscopic images of PCU and microspheres. The inset indicates a magnified picture of microspheres. Pure PCU microspheres were opaque and white, while Fe_3O_4/PCU microspheres were opaque and dark brown. All were regularly spherical however provided large size distribution. ii) Digital photos demonstrating magnetic response. When placed near a magnet, pure PCU microspheres showed no alternation, whereas composites were attracted by the magnet. Magnetic response was greater for microspheres having higher Fe_3O_4 loading. Reproduced with permission.[166] Copyright 2022, American Chemical Society. c–i) Digital photograph for subcutaneous implantation procedure on the back of a rat. ii) Gross observation for skin tissue after 2 weeks of implantation of polymer films. The tissue surrounding implanted polymers was not swollen and no severe tissue response was observed. White PCU and black Fe_3O_4/PCU biostable polymer films adhered to the tissue. iii) Histological images of hematoxylin and eosin-stained tissue sections achieved 1, 2, and 4 weeks after implantation. Red asterisks denote regions of implanted polymer. Yellow arrows indicate inflammatory cells and white arrows indicate blood vessels. No acute inflammatory reactions were seen. One week after surgery, there was a mild inflammatory infiltration in the area adjacent to implanted films, in which few inflammatory cells can be seen (yellow arrows), particularly 15% Fe/PCU. Irregular and loose connective tissues are also seen, with numerous formed blood vessels (white arrows) in these groups. At two weeks, there were fewer inflammatory cells and denser connective tissue near implanted Fe_3O_4/PCU. No inflammation signs were observed in the PCU group. Four weeks after implantation, fibrous capsules with a few inflammatory cells were seen in the surrounding area. In capsules, organized collagen fibers, and elongated fibroblasts were parallel to the polymer surface. Inflammatory reaction in the PCU group was much less than in composite groups, however, no important distinction can be seen among groups by various Fe_3O_4 loading (10, 15, and 20%). Reproduced with permission.[166] Copyright 2022, American Chemical Society.

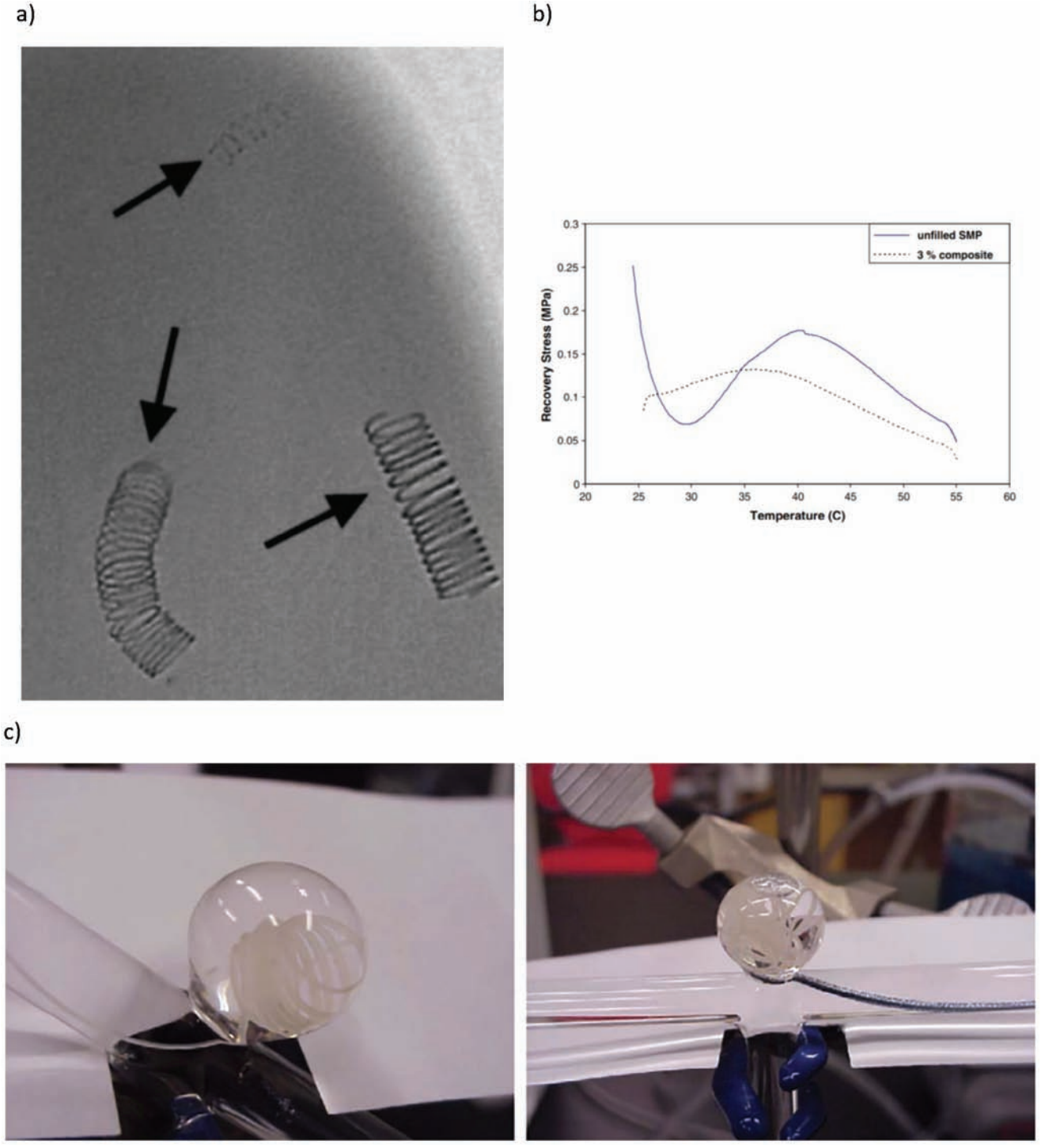

Figure 19. a) Fluoroscopic view for SMP coils having 3% tantalum of various diameters immersed in water. Coils possessed 10 mm coil diameters, and wire diameters of 0.25 (top), 0.45 (bottom left), and 0.088 mm (bottom right). Reproduced with permission.[3] Copyright 2005, Elsevier B.V. b) Recovery stress results for unfilled and filled SMP. Reproduced with permission.[3] Copyright 2005, Elsevier B.V. c) Deployment of SMP coils for aneurysm occlusion. Reproduced with permission.[3] Copyright 2005, Elsevier B.V.

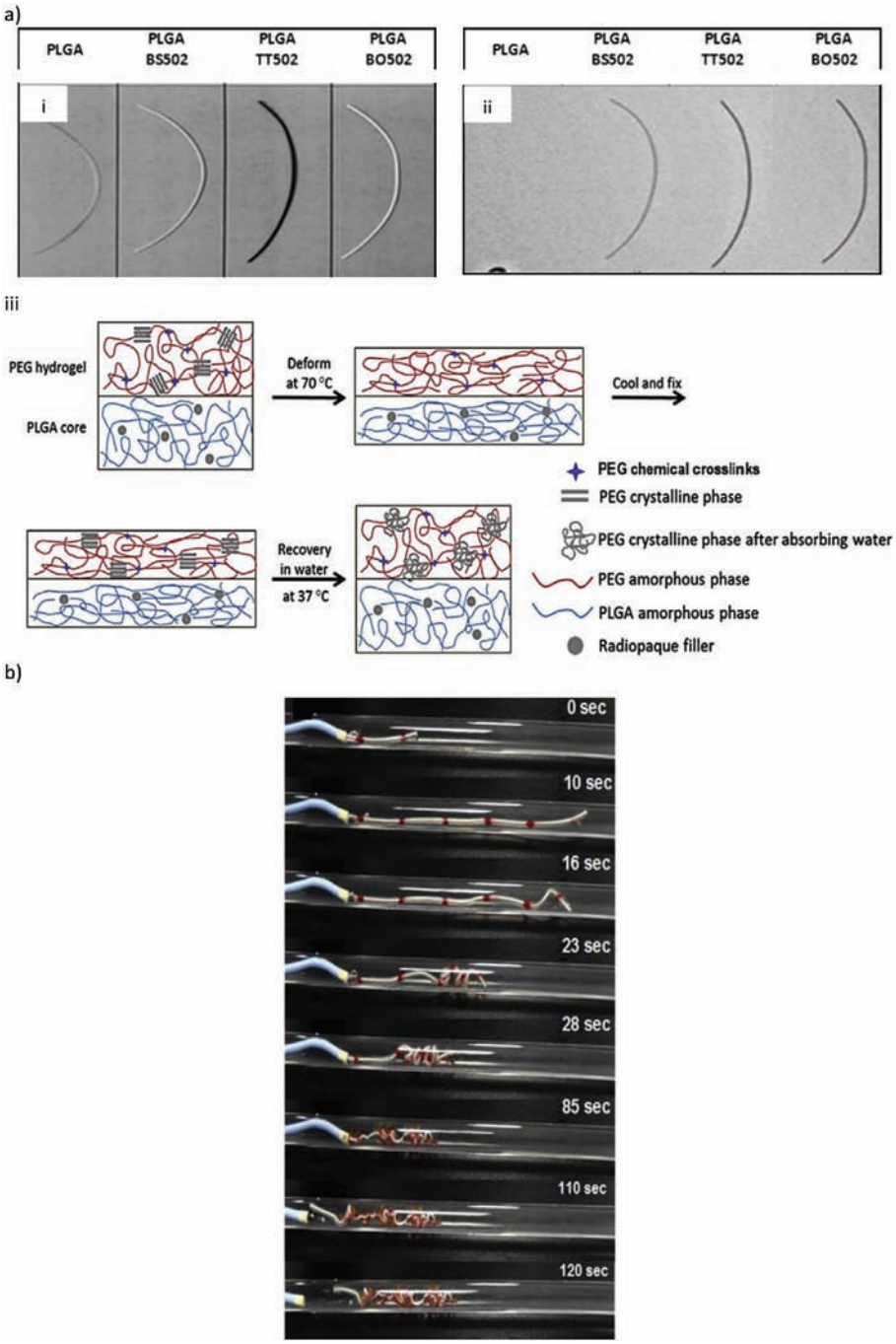

Figure 20. a–i) Optic and a–ii) radiographic images for PLGA filaments for various radiopaque content (PLGA: 100 wt% PLGA; PLGA-BS502: 48 wt% PLGA, 2 wt% PEG, 50 wt% $BaSO_4$; PLGA-TT502: 48 wt% PLGA, 2 wt% PEG, 50 wt% Ta; PLGA-BO502: 48 wt% PLGA, 2 wt% PEG, 50 wt% BO). iii) Schematic representation of water-induced shape memory mechanism for embolic device. Molecular entanglement in PLGA and covalent crosslinks in PEGDA hydrogel are netpoints responsible for maintaining permanent form and straight rod form. Programming at 70 °C, higher than the melting temperature for the PEG crystal phase, PEG and PLGA are amorphous and deformable, enabling molecular chains to be oriented across deformation direction and associated loss of entropy. The temporary deformed form is fixed with recrystallization of PEG and transition of PLGA to a glassy state when the temperature is decreased to room temperature. PEG crystallites behave as reversible switch points that drive shape recovery of PEGDA along with the swelling after immersion at 37 °C, where water molecules diffuse in the system and the network becomes completely amorphous when the PEG crystal phase "dissolves". Similarly, as PEGDA hydrogel softens sufficiently, PLGA molecular chains resume mobility and trigger recovery of PLGA shape. The water-responsive shape recovery mechanism for PLGA-PEGDA hydrogel provides the formation of an embolic plug capable of achieving complete occlusion in vitro in 120 s. The recovering form of the PLGA core facilitates the formation of an embolic plug and also provides mechanical integrity and radiopacity. Reproduced with permission.[167] Copyright 2016, Elsevier Ltd. b) In vitro embolization with embolic plug employing a flow model to simulate blood flow along the artery. After the device was deployed by 4-F catheter (at 0 s), water molecules began to diffuse in the system, actuating recovery of hydrogel coating. At 120 s, complete embolization was observed. Reproduced with permission.[167] Copyright 2016, Elsevier Ltd.

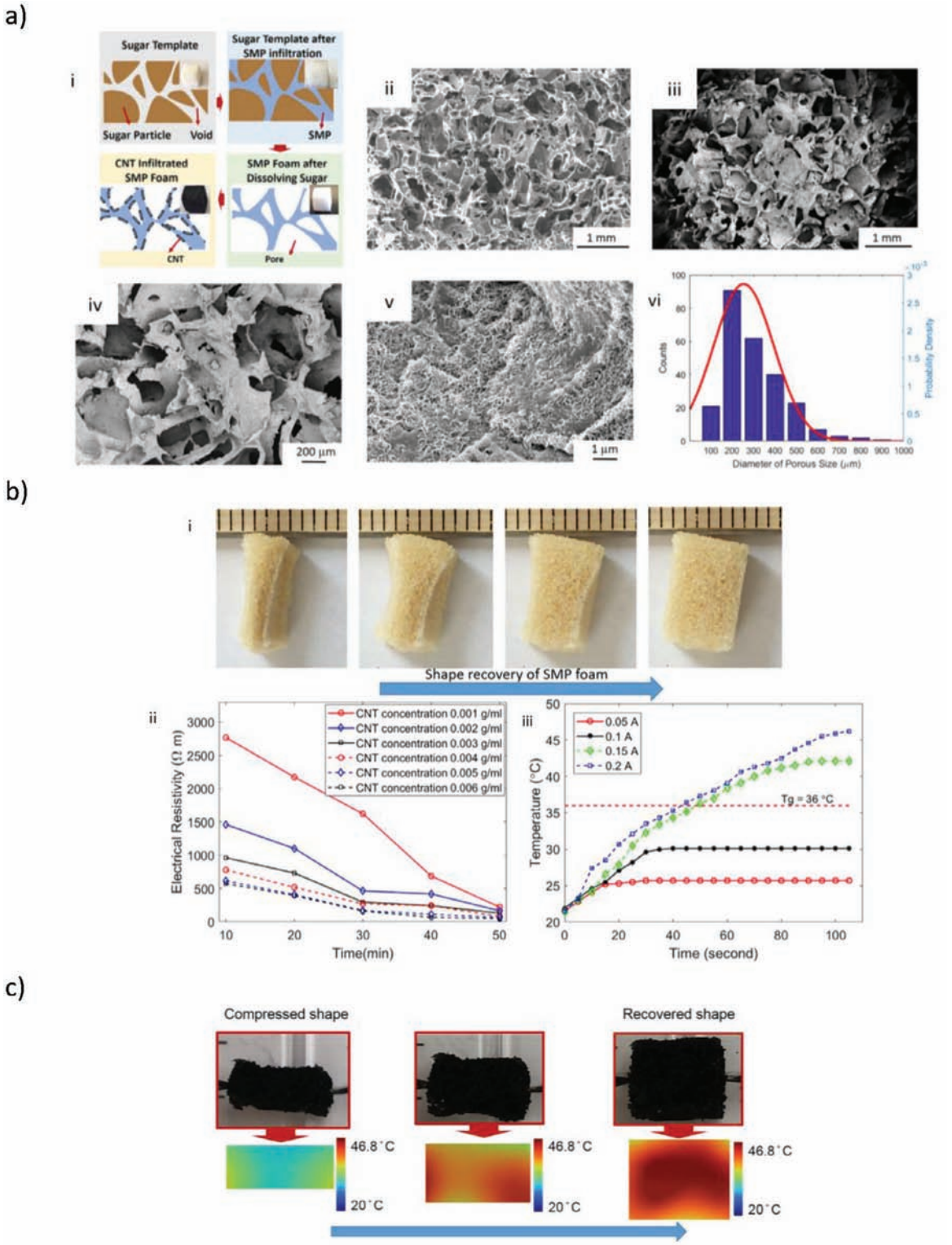

Figure 21. a) Fabrication and characterization of CNT/SMP nanocomposites. i) Fabrication scheme for CNT/SMP nanocomposites. ii) SEM micrograph for pristine SMP foam. iii–v) SEM micrographs for CNT-enhanced nanocomposites at various magnifications. vi) Pore size and distribution for SMP foam achieved by ImageJ. Reproduced with permission.[169] Copyright 2019, Elsevier B.V. b) Shape recovery for SMP foam, electrical resistivity and surface temperature for CNT/SMP nanocomposites. i) Shape recovery for pristine SMP foam on a hot plate (60 °C). ii) Influences of ultrasonication time and CNT amount on electrical resistivity for nanocomposites. iii) Temperature for CNT/SMP nanocomposites when resistive heating. Reproduced with permission.[169] Copyright 2019, Elsevier B.V. c) Shape recovery for compressed CNT/SMP nanocomposite foam via a resistive-heating technique. Reproduced with permission.[169] Copyright 2019, Elsevier B.V.

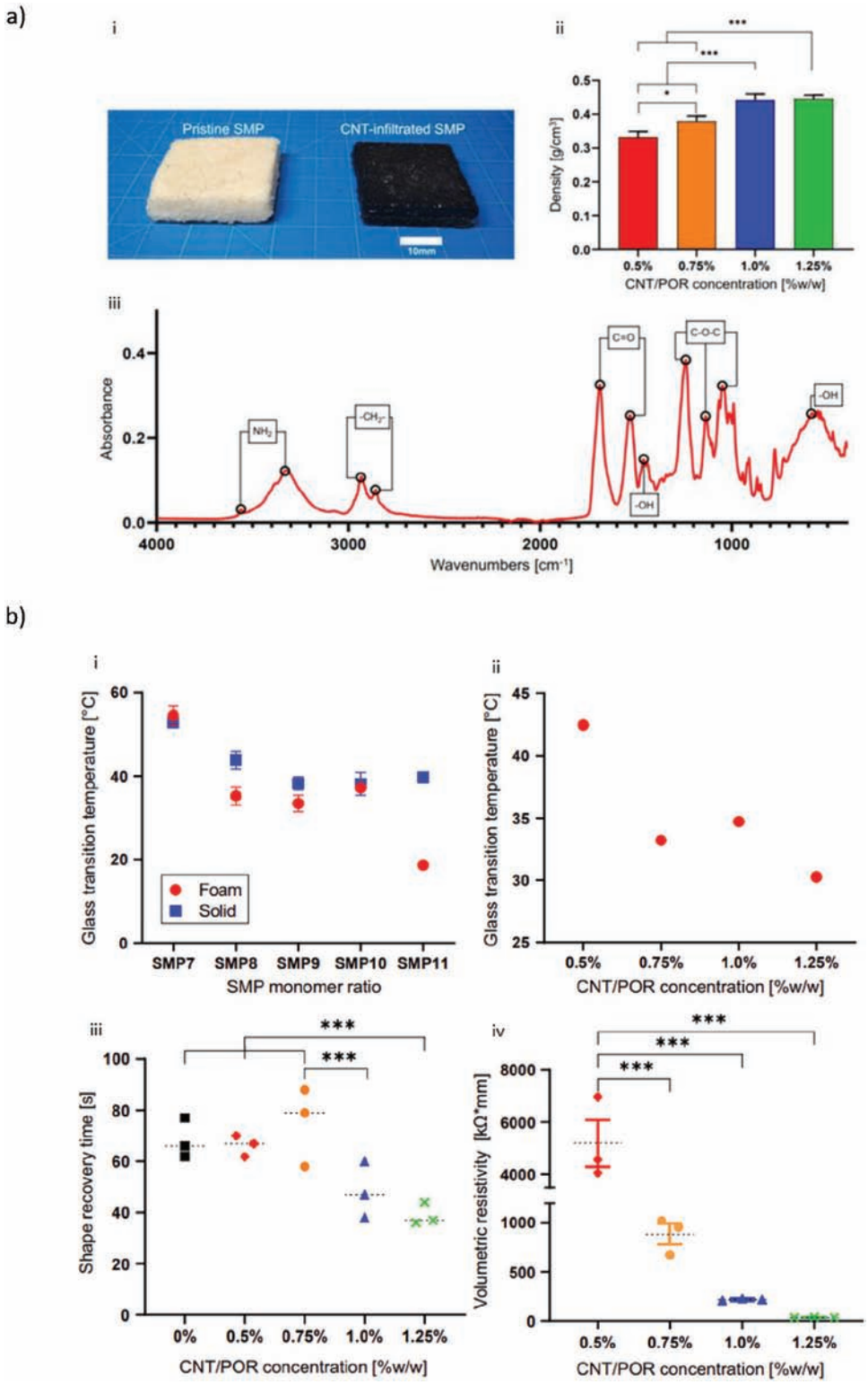

Figure 22. a) i) Photographs for pristine SMP foam (left) and CNT-infiltrated SMP foam (right) cubic samples (30 × 30 × 10 mm). ii) Density for CNT-infiltrated foams at different CNT/POR (porogen). iii) ATR-FTIR for synthesized pristine aliphatic PU SMP. Reproduced with permission.[170] Copyright 2021, Wiley-VCH GmbH. b) T_g results after DSC for (i) pristine SMP at varying monomer ratios (SMP11 is the target ratio). ii) Porous CNT-infiltrated SMP foams at different CNT/POR. Results for iii) shape recovery time of CNT-infiltrated SMP foams at different CNT/POR. iv) Volumetric resistivity. Reproduced with permission.[170] Copyright 2021, Wiley-VCH GmbH. c) Results for cyclic compression tests at T_g of i) pristine and ii) CNT-infiltrated SMP foams. iii) Cumulative stress drops for pristine and CNT-infiltrated SMP foams at different CNT/POR after tests, showing stress relaxation. (*** indicates $p < 0.001$, and * denotes $p < 0.05$). Reproduced with permission.[170] Copyright 2021, Wiley-VCH GmbH.

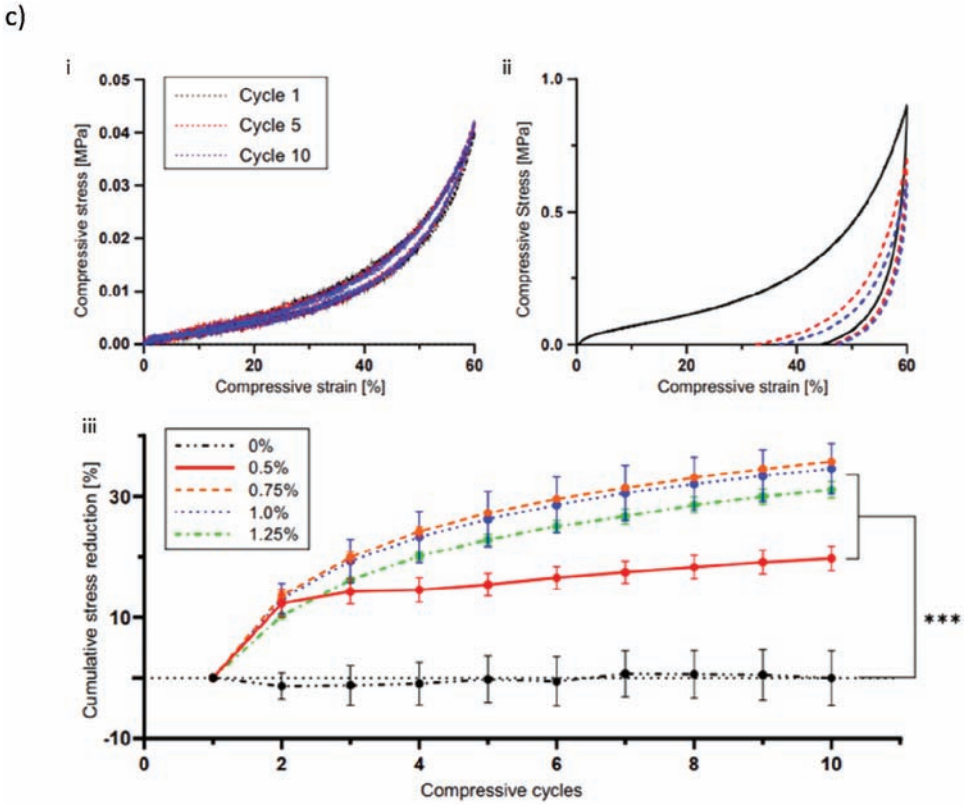

Figure 22. *Continued*

during the 1st cycle and more than 90% was recovered during the 2nd recovery cycle. The tensile strength of composites diminished by increment of filler concentration because of agglomeration and void in composites. Radiopacity of composites increased by filler concentration, where $BaSO_4$ was dominant as compared with HaP nanoparticles. Thus, fabricated hybrid nanocomposites could be used as embolic agents for interventional radiology technology because of appropriate actuation, radiopacity, and mechanical properties.[18]

Polymer composites employed in endovascular embolization are presented in **Table 5**.

6. Summary and Perspectives

Several techniques have been introduced to treat intracranial aneurysms, including platinum coil filling, stent, liquid polymer injection, polymer coil, SMPs, and metal-polymer coil combinations, each with benefits and limitations. However, all these devices seek to enhance device/thrombus stability, biocompatibility, greater volume occlusion, and enhanced compliance while decreasing adverse effects.

GDC coil was the first FDA-approved coil for the treatment of intracranial aneurysms and recurrence rate was < 30%, the mortality rate was 8%, and was not suitable to treat wide-neck aneurysms. Liquid polymer embolics provide benefits over metallic coil such as injecting a controlled amount of polymer required to completely fill the aneurysm, minimizing prolapse of the device into the vessel lumen, and minimal stress applied to the aneurysm sac. But the inability of the solidified polymer to be repositioned or retrieved after delivery, and a high rate of device migration in the parent vessel are some limitations of liquid polymer embolics. Hybrid coils are designed to address some of the problems related to metal coils, such as weak aneurysm filling and tissue response while retaining the mechanical and radiopaque benefits of platinum coil. Hydrogel coil contains coating expanding with blood, rising volumetric filling of aneurysm in comparison with bare platinum coils. Hydrogels can be a good option as a long-term embolic agent for intracranial aneurysm. However, hydrogels do not provide an important promotion in tissue response and possess short working times; furthermore, hydrogel has the potential to swell prior to the device being properly positioned into the aneurysm. Bioactive and biodegradable coils contain a polymer that elicits a cellular response to promote the fast formation of clots and endothelialization. However, the outer polymer degrades faster than the time needed for an organized thrombus to occur, causing incomplete filling and aneurysm recanalization. SMPs for intracranial aneurysm treatment can enhance existing approaches to aneurysm embolization by decreasing residual flow and preventing aneurysm recurrence. In summary, the mentioned materials attempt to enhance results by employing polymers, lower invasive processes, greater aneurysm volume filling, and materials with mechanical characteristics closer to native vessel properties.

Liquid embolics solidifying in situ are extensively being investigated. They are a good choice because of their capability to penetrate deep into the vascular system and entirely fill vascular space.

Table 5. Polymer composites used for aneurysm occlusion in the literature.

Polymer composite	Form	Characteristics	Highlighted results	Reference(s)
PU+3% tantalum filler	Composite coil	* Radiopaque	* Actuation at 32–35 °C. * Applicability showed in vitro * Visible with traditional imaging.	[3]
PU+4% tungsten filler	Foam composite	* Biocompatible * High porosity * Low density	* Applicability showed in vitro. * Enhanced radiopacity.	[15]
CNT/SMP (Three monomers: i) HDI, ii) HPED, iii) TEA were utilized to synthesize SMP)	Porous foam	* Flexibility * High porosity * Good shape recovery	* Resistive-heating activation mechanism is designed to trigger shape recovery due to the ease of implementation of mechanism.	[169]
Hybrid composites ($BaSO_4$ and HaP in PU SMP matrix). Pure SMP dispersed with 4, 10, and 12.5 wt% concentration of nano $BaSO_4$, nano-HaP added at concentration of 2.5%, 5%, 7.5%, and 10 wt% in SMP hybrid composites. for individual filler concentration of 7.5 wt% HaP/2.5 wt% $BaSO_4$, 5 wt% HaP/5 wt% $BaSO_4$, and 2.5 wt% HaP/7.5 wt% $BaSO_4$.	-	* Temperature-activated	* Shape recovery properties of hybrid nanocomposites reduced. * Tensile strength of composites diminished by increment in filler concentration. * Radiopacity of composites increased with filler concentration. * Hybrid PU SMP/HaP/$BaSO_4$ nanocomposites could be used as embolic agents in interventional radiology method.	[18]

Future direction should focus on enhanced effectiveness and decreased toxicity. While the first-generation liquid embolics Onyx and Trufill possess toxic byproducts, most of new generation ones show low or no cytotoxicity. Trends in liquid embolics will be the capability to deliver one or more therapeutic agents locally to the aimed site while restricting blood flow.

The use of polymeric materials in coils can provide less toxicity and better biocompatibility when compared to metallic coils. However, most polymers are radiolucent and not visible on traditional imaging methods. The addition of radiopaque agents such as tantalum or tungsten can increase tracking in diagnostic imaging and monitoring of catheterization processes.

Multiple design criteria should be considered in the design of materials used for endovascular embolization of intracranial aneurysms including biodegradability, compliance, and radiopacity.

Current research shows that polymeric devices enhance volumetric filling and subsequent stabilization of aneurysms, resulting in better patient results and lower morbidity and mortality rates. While the usage of polymers, polymeric blends, and polymeric composites is conceptually promising, further clinical work will be required to ensure the applicability of polymeric materials in clinical settings.

In summary, intracranial aneurysm treatment has shifted from complex open surgical access methods to minimally invasive endovascular techniques, with growth in imaging and material science areas in recent years. Advances in the development of novel polymeric materials can help the therapy of intracranial aneurysms with minimum side effects. Therefore, future studies should focus on the development of new polymeric materials. Future works may also consist of histological observation of tissue collected at the operating site at different post-treatment time points to evaluate the extent of injury.

Employing polymeric materials, it is possible to design unique materials that can be implemented in other applications beyond interventional embolization of intracranial aneurysms such as cardiovascular implants (ranging from coronary stents to tissue-engineered constructs),[149,171,172] left atrial appendage occluders,[173] biomedical implants (e.g., bone fixation, bone screws),[174] and so on.

Acknowledgements

All authors contributed equally to this work.

Conflict of Interest

The authors declare no conflict of interest.

Keywords

endovascular embolization, intracranial aneurysms, polymer blends, polymer composites, polymers

Received: September 22, 2023
Revised: November 3, 2023
Published online: November 22, 2023

[1] W. I. Schievink, *N. Engl. J. Med.* **1997**, *336*, 28.
[2] R. Kunkel, D. Laurence, J. Wang, D. Robinson, J. Scherrer, Y. Wu, B. Bohnstedt, A. Chien, Y. Liu, C.-H. Lee, *J. Mech. Behav. Biomed. Mater.* **2018**, *88*, 422.

[3] J. M. Hampikian, B. C. Heaton, F. C. Tong, Z. Zhang, C. P. Wong, *Mater. Sci. Eng., C* **2006**, *26*, 1373.
[4] R. L. Sacco, P. A. Wolf, N. E. Bharucha, S. L. Meeks, W. B. Kannel, L. J. Charette, P. M. Mcnamara, E. P. Palmer, R. D'agostino, *Neurology* **1984**, *34*, 847.
[5] J. T. King Jr, *Neuroimaging Clin. North Am.* **1997**, *7*, 659.
[6] J. M. Wardlaw, P. M. White, *Brain* **2000**, *123*, 205.
[7] J. B. Bederson, E. S. Connolly, H. H. Batjer, R. G. Dacey, J. E. Dion, M. N. Diringer, J. E. Duldner, R. E. Harbaugh, A. B. Patel, R. H. Rosenwasser, *Stroke* **2009**, *40*, 994.
[8] E. S. Connolly, A. A. Rabinstein, J. R. Carhuapoma, C. P. Derdeyn, J. Dion, R. T. Higashida, B. L. Hoh, C. J. Kirkness, A. M. Naidech, C. S. Ogilvy, A. B. Patel, B. G. Thompson, P. Vespa, *Stroke* **2012**, *43*, 1711.
[9] N. S. Naval, T. Chang, F. Caserta, R. G. Kowalski, J. R. Carhuapoma, R. J. Tamargo, *J Crit Care* **2012**, *27*, 532.1.
[10] H. Lantigua, S. Ortega-Gutierrez, J. M. Schmidt, K. Lee, N. Badjatia, S. Agarwal, J. Claassen, E. S. Connolly, S. A. Mayer, *Crit. Care* **2015**, *19*, 309.
[11] C. Agner, M. Dujovny, *Neurol. Res.* **2009**, *31*, 632.
[12] C. Agner, M. Dujovny, *Neurol. Res.* **2009**, *31*, 560.
[13] M. Sluzewski, W. J. Van Rooij, G. N. Beute, P. C. Nijssen, *J. Neurosurg.* **2006**, *105*, 396.
[14] A. J. Molyneux, R. S. C. Kerr, L.-M. Yu, M. Clarke, M. Sneade, J. A. Yarnold, P. Sandercock, *Lancet* **2005**, *366*, 809.
[15] J. N. Rodriguez, Y.-J. Yu, M. W. Miller, T. S. Wilson, J. Hartman, F. J. Clubb, B. Gentry, D. J. Maitland, *Ann. Biomed. Eng.* **2012**, *40*, 883.
[16] T. H. Lee, T. Y. Kim, K. Rhee, J. Y. Jho, *Macromol. Res.* **2018**, *26*, 634.
[17] W. Brinjikji, D. F. Kallmes, R. Kadirvel, *Am. J. Neuroradiol.* **2015**, *36*, 1216.
[18] D. Kashyap, S. S. Gaur, S. Kanagaraj, *Mater. Today Commun.* **2020**, *22*, 100751.
[19] J. M. Acosta, A. F. Cayron, N. Dupuy, G. Pelli, B. Foglia, J. Haemmerli, E. Allémann, P. Bijlenga, B. R. Kwak, S. Morel, *Front. Cardiovasc. Med.* **2021**, *8*, 775307.
[20] J. Zhao, H. Lin, R. Summers, M. Yang, B. G. Cousins, J. Tsui, *Angiology* **2018**, *69*, 17.
[21] H. R. Jarrah, A. Zolfagharian, M. Bodaghi, *Biomech. Model. Mechanobiol.* **2022**, *21*, 383.
[22] S. A. Pineda-Castillo, A. M. Stiles, B. N. Bohnstedt, H. Lee, Y. Liu, C.-H. Lee, *Polymers* **2022**, *14*, 2526.
[23] E. A. Winkler, A. Lee, J. K. Yue, K. P. Raygor, W. C. Rutledge, R. R. Rubio, S. A. Josephson, M. S. Berger, D. M. S. Raper, A. A. Abla, *Acta Neurochir.* **2021**, *163*, 1527.
[24] C. Wang, M. Li, H. Chen, X. Yang, Y. Zhang, D. Zhang, *J. Neurointerventional Surg.* **2022**, *14*, 734.
[25] G. Guglielmi, F. Viñuela, J. Dion, G. Duckwiler, *J. Neurosurg.* **1991**, *75*, 8.
[26] J. Raymond, A. Metcalfe, A.-C. Desfaits, E. Ribourtout, I. Salazkin, K. Gilmartin, G. Embry, R. J. Boock, *Am. J. Neuroradiol.* **2003**, *24*, 1214.
[27] G. Guglielmi, F. Viñuela, I. Sepetka, V. Macellari, *J. Neurosurg.* **1991**, *75*, 1.
[28] G. Guglielmi, F. Viñuela, G. Duckwiler, J. Dion, P. Lylyk, A. Berenstein, C. Strother, V. Graves, V. Halbach, D. Nichols, N. Hopkins, R. Ferguson, I. Sepetka, *J. Neurosurg.* **1992**, *77*, 515.
[29] G. Guglielmi, *J. Stroke Cerebrovasc. Dis.* **1997**, *6*, 246.
[30] K. Mori, Y. Nakao, N. Horinaka, R. Wada, A. Hirano, M. Maeda, *Neurol. Med.–Chir.* **2003**, *43*, 293.
[31] A. F. Zubillaga, G. Guglielmi, F. Viñuela, G. R. Duckwiler, *Am. J. Neuroradiol.* **1994**, *15*, 815.
[32] T. W. Malisch, G. Guglielmi, F. Viñuela, G. Duckwiler, Y. P. Gobin, N. A. Martin, J. G. Frazee, *J. Neurosurg.* **1997**, *87*, 176.
[33] G. Bavinzski, V. Talazoglu, M. Killer, B. Richling, A. Gruber, C. E. Gross, H. Plenk, *J. Neurosurg.* **1999**, *91*, 284.
[34] M. Sluzewski, T. Menovsky, W. J. van Rooij, D. Wijnalda, *Am. J. Neuroradiol.* **2003**, *24*, 257.
[35] M. M. Taha, I. Nakahara, T. Higashi, Y. Iwamuro, M. Iwaasa, Y. Watanabe, K. Tsunetoshi, T. Munemitsu, *Surg. Neurol.* **2006**, *66*, 277.
[36] A. J. Molyneux, R. S. Kerr, J. Birks, N. Ramzi, J. Yarnold, M. Sneade, J. Rischmiller, *Lancet Neurol.* **2009**, *8*, 427.
[37] J. K. A. Hope, J. V. Byrne, A. J. Molyneux, *Am. J. Neuroradiol.* **1999**, *20*, 391.
[38] S. Tateshima, Y. Murayama, Y. P. Gobin, G. R. Duckwiler, G. Guglielmi, F. Viñuela, *Neurosurgery* **2000**, *47*, 1332.
[39] J.-N. Vallée, A. Aymard, E. Vicaut, M. Reis, J.-J. Merland, *Radiology* **2003**, *226*, 867.
[40] J. C. Wehman, R. A. Hanel, E. I. Levy, L. N. Hopkins, *Neurosurgery* **2006**, *59*, S3.
[41] D. F. Kallmes, N. H. Fujiwara, *Am. J. Neuroradiol.* **2002**, *23*, 1580.
[42] P. M. White, S. C. Lewis, A. Gholkar, R. J. Sellar, H. Nahser, C. Cognard, L. Forrester, J. M. Wardlaw, *Lancet* **2011**, *377*, 1655.
[43] A. Williams, J. Millar, A. Ditchfield, S. Vundavalli, S. Barker, *Interventional Neuroradiol.* **2014**, *20*, 37.
[44] X.-B. Guo, Y.-M. Fan, J.-N. Zhang, *Eur. J. Radiol.* **2011**, *79*, 42.
[45] A. J. Boyle, M. A. Wierzbicki, S. Herting, A. C. Weems, A. Nathan, W. Hwang, D. J. Maitland, *Med. Eng. Phys.* **2017**, *49*, 56.
[46] W. J. Van Rooij, M. Sluzewski, *Am. J. Neuroradiol.* **2007**, *28*, 1405.
[47] H. J. Cloft, G. J. Joseph, F. C. Tong, J. H. Goldstein, J. E. Dion, *Am. J. Neuroradiol.* **2000**, *21*, 1312.
[48] H. J. Cloft, *Am. J. Neuroradiol.* **2006**, *27*, 289.
[49] M. Killer, T. Hauser, A. Wenger, B. Richling, G. Ladurner, *Acta Neurochir.* **2009**, *151*, 497.
[50] J. H. Park, H.-S. Kang, M. H. Han, P. Jeon, D.-S. Yoo, T. H. Lee, *Am. J. Neuroradiol.* **2011**, *32*, 1756.
[51] M. Killer, D. F. Kallmes, M. R. McCoy, Y.-H. Ding, J. C. Shum, G. M. Cruise, *Am. J. Neuroradiol.* **2009**, *30*, 1488.
[52] M. J. Constant, E. M. Keeley, G. M. Cruise, *J. Biomed. Mater. Res., Part B* **2009**, *89*, 306.
[53] M. R. Mccoy, G. M. Cruise, M. Killer, *Eur. Radiol.* **2010**, *20*, 870.
[54] M. Killer, M. R. Mccoy, M. C. Vestal, L. Weitgasser, G. M. Cruise, *Am. J. Neuroradiol.* **2011**, *32*, 923.
[55] D. F. Kallmes, N. H. Fujiwara, D. Yuen, D. Y. Dai, S. T. Li, *Am. J. Neuroradiol.* **2003**, *24*, 591.
[56] T. Gunnarsson, P. Klurfan, K. G. Terbrugge, R. A. Willinsky, *Can. J. Neurol. Sci.* **2007**, *34*, 38.
[57] A. S. Arthur, S. A. Wilson, S. Dixit, J. D. Barr, *Neurosurg Focus* **2005**, *18*, 1.
[58] J. Ortega, D. Maitland, T. Wilson, W. Tsai, Ö. Savas, D. Saloner, *Ann. Biomed. Eng.* **2007**, *35*, 1870.
[59] K. Kinugasa, S. Mandai, Y. Terai, I. Kamata, K. Sugiu, T. Ohmoto, A. Nishimoto, *J. Neurosurg.* **1992**, *77*, 501.
[60] K. Kinugasa, S. Mandai, S. Tsuchida, K. Sugiu, I. Kamata, K. Tokunaga, T. Ohmoto, K. Taguchi, *Neurosurgery* **1994**, *34*, 694.
[61] R. Loch Macdonald, S. Mojtahedi, L. Johns, A. Kowalczuk, *Stroke* **1998**, *29*, 478.
[62] X. Yang, Z. Wu, Y. Li, J. Tang, Y. Sun, Z. Liu, K. Yin, *Surg. Neurol.* **2001**, *55*, 116.
[63] P. Mordasini, A. K. Kraehenbuehl, J. V. Byrne, S. Vandenberghe, M. Reinert, H. Hoppe, J. Gralla, *Am. J. Neuroradiol.* **2013**, *34*, 2177.
[64] I. M. Germano, R. L. Davis, C. B. Wilson, G. B. Hieshima, *J. Neurosurg.* **1992**, *76*, 607.
[65] M. Guimaraes, D. Arrington, T. MacFall, R. Yamada, C. Schönholz, *Endovasc. Today* **2013**, 70.
[66] M. M. Jensen, Ø. Hatlevik, D. D. Steinhauff, E. D. Griswold, X. Wei, K. J. Isaacson, Z. B. Barber, E. Huo, P. Taussky, J. Jedrzkiewicz, J. Cappello, D. Cheney, H. Ghandehari, *Acta Biomater.* **2022**, *151*, 174.
[67] F. Mottu, P. Gailloud, D. Massuelle, D. A. Rüfenacht, E. Doelker, *Biomaterials* **2000**, *21*, 803.

[68] Y. Yonekawa, Y. Kaku, H. Iwata, in *New Trends in Management of Cerebro-Vascular Malformations* (Eds.: A. Pasqualin, R. Pian), Springer, Vienna **1994**.
[69] G. M. Debrun, V. Aletich, J. I. Ausman, F. Charbel, M. Dujovny, *Neurosurgery* **1997**, *40*, 112.
[70] H. I. Farhat, M. S. Elhammady, M. A. Aziz-Sultan, *Neurosurgery* **2010**, *67*, E216.
[71] W. Gombotz, *Adv. Drug Delivery Rev.* **1998**, *31*, 267.
[72] T. A. Becker, D. R. Kipke, T. Brandon, *J. Biomed. Mater. Res.* **2001**, *54*, 76.
[73] T. A. Becker, D. R. Kipke, *J. Biomed. Mater. Res.* **2002**, *61*, 533.
[74] B. Jeong, S. W. Kim, Y. H. Bae, *Adv. Drug Delivery Rev.* **2002**, *54*, 37.
[75] H. H. Tønnesen, J. Karlsen, *Drug Dev. Ind. Pharm.* **2002**, *28*, 621.
[76] O. Jordan, E. Doelker, D. A. Rüfenacht, *Cardiovasc. Interventional Radiol.* **2005**, *28*, 561.
[77] B. Vernon, A. Martinez, *J. Biomater. Sci., Polym. Ed.* **2005**, *16*, 1153.
[78] V. Cheng, B. H. Lee, C. Pauken, B. L. Vernon, *J. Appl. Polym. Sci.* **2007**, *106*, 1201.
[79] S. Vaidya, K. Tozer, J. Chen, *Semin. Interventional Radiol.* **2008**, *25*, 204.
[80] B. P. Barnett, A. H. Hughes, S. Lin, A. Arepally, P. H. Gailloud, *J. Vasc. Interventional Radiol.* **2009**, *20*, 507.
[81] H. H. Bearat, B. H. Lee, J. Valdez, B. L. Vernon, *J. Biomater. Sci., Polym. Ed.* **2011**, *22*, 1299.
[82] H. H. Bearat, M. C. Preul, B. L. Vernon, *J. Biomed. Mater. Res., Part A* **2013**, *101*, 2515.
[83] B. P. Barnett, P. Gailloud, *J. Vasc. Interventional Radiol.* **2011**, *22*, 203.
[84] Z. Cui, B. H. Lee, C. Pauken, B. L. Vernon, *J. Biomed. Mater. Res., Part A* **2011**, *98*, 159.
[85] B. H. Lee, C. Leon, R. Mclemore, J. V. Macias, B. L. Vernon, *J. Biomater. Sci., Polym. Ed.* **2011**, *22*, 2357.
[86] C. M. Riley, R. Mclemore, M. C. Preul, B. L. Vernon, *J. Biomed. Mater. Res., Part B* **2011**, *96*, 47.
[87] C. R. Brennecka, M. C. Preul, W. D. Bichard, B. L. Vernon, *World Neurosurg.* **2012**, *78*, 469.
[88] C. R. Brennecka, M. C. Preul, B. L. Vernon, *J. Biomed. Mater. Res., Part B* **2012**, *100*, 1298.
[89] C. R. Brennecka, M. C. Preul, T. A. Becker, B. L. Vernon, *J. Neurosurg.* **2013**, *119*, 228.
[90] S. N. Pawar, K. J. Edgar, *Biomaterials* **2012**, *33*, 3279.
[91] O. Dudeck, O. Jordan, K. T. Hoffmann, A. F. Okuducu, I. Husmann, T. Kreuzer-Nagy, K. Tesmer, P. Podrabsky, H. Bruhn, J. Hilborn, D. A. Rüfenacht, E. Doelker, R. Felix, *Am. J. Neuroradiol.* **2006**, *27*, 1849.
[92] A. Poursaid, M. M. Jensen, E. Huo, H. Ghandehari, *J. Controlled Release* **2016**, *240*, 414.
[93] T. A. Becker, M. C. Preul, W. D. Bichard, D. R. Kipke, C. G. Mcdougall, *Neurosurgery* **2005**, *56*, 793.
[94] T. A. Becker, M. C. Preul, W. D. Bichard, D. R. Kipke, C. G. Mcdougall, *Neurosurgery* **2007**, *60*, 1119.
[95] H. Takao, Y. Murayama, T. Saguchi, T. Ishibashi, M. Ebara, K. Irie, H. Yoshioka, Y. Mori, S. Ohtsubo, F. Viñuela, T. Abe, *Interventional Neuroradiol.* **2006**, *12*, 154.
[96] H. H. Bearat, *Ph.D.*, Arizona State University, **2012**.
[97] X. Chen, T. Taguchi, *Polym. J.* **2020**, *52*, 793.
[98] O. Poupart, R. Conti, A. Schmocker, L. Pancaldi, C. Moser, K. M. Nuss, M. S. Sakar, T. Dobrocky, H. Grützmacher, P. J. Mosimann, D. P. Pioletti, *Front. Bioeng. Biotechnol.* **2021**, *8*, 619858.
[99] J. N. Rodriguez, W. Hwang, J. Horn, T. L. Landsman, A. Boyle, M. A. Wierzbicki, S. M. Hasan, D. Follmer, J. Bryant, W. Small, D. J. Maitland, *J. Biomed. Mater. Res., Part A* **2015**, *103A*, 1577.
[100] L. Wang, S. Wu, G. Cao, Y. Fan, N. Dunne, X. Li, *J. Mater. Chem. B* **2019**, *7*, 7439.
[101] J. Wu, C. Hu, Z. Tang, Q. Yu, X. Liu, H. Chen, *Colloid Interface Sci. Commun.* **2018**, *23*, 34.
[102] A. Tortoriello, G. Pedrizzetti, *J. Biomech.* **2004**, *37*, 1.
[103] L. Morris, F. Stefanov, T. Mcgloughlin, *J. Biomech.* **2013**, *46*, 383.
[104] H. Kamata, X. Li, U.-I.. Chung, T. Sakai, *Adv. Healthcare Mater.* **2015**, *4*, 2360.
[105] O. Poupart, A. Schmocker, R. Conti, C. Moser, K. M. Nuss, H. Grützmacher, P. J. Mosimann, D. P. Pioletti, *Front. Bioeng. Biotechnol.* **2020**, *8*, 261.
[106] G. Girdhar, M. Read, J. Sohn, C. Shah, S. Shrivastava, *J. Neurol. Sci.* **2014**, *339*, 97.
[107] F. Xu, K. Hart, C. E. Flanagan, J. C. Nacker, R. Moftakhar, B. Aagaard-Kienitz, D. W. Consigny, J. R. Grinde, W. C. Crone, K. S. Masters, *J. Med. Devices* **2009**, *3*, 045001.
[108] R. I. Mehta, R. I. Mehta, M. C. Fishbein, O. E. Solis, R. Jahan, N. Salamon, H. V. Vinters, W. H. Yong, *Hum. Pathol.* **2009**, *40*, 1803.
[109] J. M. Abrahams, S. L. Diamond, R. W. Hurst, E. L. Zager, M. S. Grady, *Surg. Neurol.* **2000**, *54*, 34.
[110] M. H. Babiker, L. F. Gonzalez, F. Albuquerque, D. Collins, A. Elvikis, C. Zwart, B. Roszelle, D. H. Frakes, *IEEE Trans. Biomed. Eng.* **2013**, *60*, 1150.
[111] S. Geyik, O. Ertugrul, K. Yavuz, P. Geyik, I. Saatci, H. S. Cekirge, *J. Neurosurg.* **2010**, *112*, 709.
[112] M. Bendszus, L. Solymosi, *Am. J. Neuroradiol.* **2006**, *27*, 2053.
[113] D. Fiorella, F. C. Albuquerque, C. G. Mcdougall, *Neurosurgery* **2006**, *58*, 51.
[114] S. A. Ansari, E. J. Dueweke, Y. Kanaan, N. Chaudhary, D. Gandhi, B. G. Thompson, J. J. Gemmete, *J. Neurointerventional Surg.* **2011**, *3*, 324.
[115] Q. Wang, Y. Gao, X. Sun, B. Ji, X. Cui, Y. Liu, T. Zheng, C. Chen, X. Jiang, A. Zhu, D. Quan, *Biomed. Mater.* **2014**, *9*, 045004.
[116] O. Rukovets, *Neurol. Today* **2011**, *11*, 24.
[117] E. Veznedaroglu, C. J. Koebbe, A. Siddiqui, R. H. Rosenwasser, *Neurosurgery* **2008**, *62*, 799.
[118] M. Piotin, S. Pistocchi, B. Bartolini, R. Blanc, *Neuroradiology* **2012**, *54*, 345.
[119] H. J. Cloft, *Am. J. Neuroradiol.* **2007**, *28*, 152.
[120] T. Gunnarsson, F. C. Tong, P. Klurfan, C. M. Cawley, J. E. Dion, *Am. J. Neuroradiol.* **2009**, *30*, 1657.
[121] H. S. Cekirge, I. Saatci, M. H. Ozturk, B. Cil, A. Arat, M. Mawad, F. Ergungor, D. Belen, U. Er, S. Turk, M. Bavbek, Z. Sekerci, E. Beskonakli, O. E. Ozcan, T. Ozgen, *Neuroradiology* **2006**, *48*, 113.
[122] R. L. Piske, L. H. Kanashiro, E. Paschoal, C. Agner, S. S. Lima, P. H. Aguiar, *Neurosurgery* **2009**, *64*, E865.
[123] W. Zhao, L. Liu, F. Zhang, J. Leng, Y. Liu, *Mater. Sci. Eng., C* **2019**, *97*, 864.
[124] D. J. Macdonald, H. M. Finlay, P. B. Canham, *Ann. Biomed. Eng.* **2000**, *28*, 533.
[125] J. D. Humphrey, S. Na, *Ann. Biomed. Eng.* **2002**, *30*, 509.
[126] D. J. Maitland, W. Small, J. M. Ortega, P. R. Buckley, J. Rodriguez, J. Hartman, T. S. Wilson, *J. Biomed. Opt.* **2007**, *12*, 030504.
[127] D. J. Maitland, M. F. Metzger, D. Schumann, A. Lee, T. S. Wilson, *Lasers Surg. Med.* **2002**, *30*, 1.
[128] H. Tobushi, H. Hara, E. Yamada, S. Hayashi, *Smart Mater. Struct.* **1996**, *5*, 483.
[129] Z. G. Wei, R. Sandstroröm, S. Miyazaki, *J. Mater. Sci.* **1998**, *33*, 3743.
[130] M. C. Serrano, G. A. Ameer, *Macromol. Biosci.* **2012**, *12*, 1156.
[131] Y. Liu, H. Du, L. Liu, J. Leng, *Smart Mater. Struct.* **2014**, *23*, 023001.
[132] D. Echeverría, R. Rivera, P. Giacaman, J. G. Sordo, M. Einersen, L. Badilla, *J. Neurointerventional Surg.* **2023**, *15*, 781.
[133] J. Horn, W. Hwang, S. L. Jessen, B. K. Keller, M. W. Miller, E. Tuzun, J. Hartman, F. J. Clubb, D. J. Maitland, *J. Biomed. Mater. Res., Part B* **2017**, *105*, 1892.
[134] S. M. Herting, Y. Ding, A. J. Boyle, D. Dai, L. D. Nash, S. Asnafi, D. R. Jakaitis, C. R. Johnson, L. M. Graul, C. Yeh, D. F. Kallmes, R. Kadirvel, D. J. Maitland, *J. Biomed. Mater. Res., Part B* **2019**, *107*, 2466.

[135] S. L. Jessen, M. C. Friedemann, A. E. Mullen, A.-M. Ginn-Hedman, S. M. Herting, D. J. Maitland, F. J. Clubb, *J. Biomed. Mater. Res., Part B* **2020**, *108*, 2238.
[136] J. N. Rodriguez, F. J. Clubb, T. S. Wilson, M. W. Miller, T. W. Fossum, J. Hartman, E. Tuzun, P. Singhal, D. J. Maitland, *J. Biomed. Mater. Res., Part A* **2014**, *102*, 1231.
[137] A. J. Boyle, T. L. Landsman, M. A. Wierzbicki, L. D. Nash, W. Hwang, M. W. Miller, E. Tuzun, S. M. Hasan, D. J. Maitland, *J. Biomed. Mater. Res., Part B* **2016**, *104*, 1407.
[138] J. Wang, R. Kunkel, J. Luo, Y. Li, H. Liu, B. N. Bohnstedt, Y. Liu, C.-H. Lee, *Polymers* **2019a**, *11*, 631.
[139] A. A. Ahuja, R. W. Hergenrother, C. M. Strother, A. A. Rappe, S. L. Cooper, V. B. Graves, *A. J. Neuroradiol.* **1993**, *14*, 794.
[140] H. Wang, B. Wang, K. P. Normoyle, K. Jackson, K. Spitler, M. F. Sharrock, C. M. Miller, C. Best, D. Llano, R. Du, *Front. Neurosci.* **2014**, *8*, 307.
[141] A. D. Muschenborn, J. M. Ortega, J. M. Szafron, D. J. Szafron, D. J. Maitland, *Biomed. Eng. Online* **2013**, *12*, 103.
[142] A. Metcalfe, A.-C. Desfaits, I. Salazkin, L. '. Yahia, W. M. Sokolowski, J. Raymond, *Biomaterials* **2003**, *24*, 491.
[143] M. Cabanlit, D. Maitland, T. Wilson, S. Simon, T. Wun, M. E. Gershwin, J. Van De Water, *Macromol. Biosci.* **2007**, *7*, 48.
[144] P. Singhal, J. N. Rodriguez, W. Small, S. Eagleston, J. Van De Water, D. J. Maitland, T. S. Wilson, *J. Polym. Sci., Part B: Polym. Phys.* **2012**, *50*, 724.
[145] G. M. Cruise, J. C. Shum, H. Plenk, *J. Mater. Chem.* **2007**, *17*, 3965.
[146] S. L. Jessen, M. C. Friedemann, A.-M. Ginn-Hedman, L. M. Graul, S. Jokerst, C. B. Robinson, T. L. Landsman, F. J. Clubb, D. J. Maitland, *ACS Biomater. Sci. Eng.* **2020**, *6*, 2588.
[147] S. M. Chau, S. M. Herting, D. A. Noltensmeyer, H. Ahmed, D. J. Maitland, S. Raghavan, *J. Biomed. Mater. Res., Part B* **2022**, *110*, 1535.
[148] W. Small, P. R. Buckley, T. S. Wilson, W. J. Benett, J. Hartman, D. Saloner, D. J. Maitland, *IEEE Trans. Biomed. Eng.* **2007**, *54*, 1157.
[149] H. W. Toh, D. W. Y. Toong, J. C. K. Ng, V. Ow, S. Lu, L. P. Tan, P. E. H. Wong, S. Venkatraman, Y. Huang, H. Y. Ang, *Eur. Polym. J.* **2021**, *146*, 110249.
[150] I. Linfante, N. M. Akkawi, A. Perlow, V. Andreone, A. K. Wakhloo, *Stroke* **2005**, *36*, 1948.
[151] Y. H. Ding, D. Dai, D. A. Lewis, H. J. Cloft, D. F. Kallmes, *Am. J. Neuroradiol.* **2005**, *26*, 1757.
[152] W. J. Van Rooij, A. N. De Gast, M. Sluzewski, *Am. J. Neuroradiol.* **2008**, *29*, 991.
[153] V. Gupta, C. D. Gandhi, C. J. Prestigiacomo, *J. Neurosurg. Sci.* **2012**, *56*, 163.
[154] Y. Murayama, S. Tateshima, N. R. Gonzalez, F. Vinuela, *Stroke* **2003**, *34*, 2031.
[155] L. E. Skolarus, J. J. Gemmete, T. Braley, L. B. Morgenstern, A. Pandey, *World Neurosurg.* **2010**, *74*, 640.
[156] H.-S. Kang, M. H. Han, B. J. Kwon, O.-K. Kwon, S. H. Kim, S. H. Choi, K.-H. Chang, *Am. J. Neuroradiol.* **2005**, *26*, 1921.
[157] S.-K. Hwang, S.-H. Kim, *Ewha Med. J.* **2012**, *35*, 38.
[158] Y. Murayama, F. Vin~Uela, S. Tateshima, N. R. Gonzalez, J. K. Song, H. Mahdavieh, L. Iruela-Arispe, *Stroke* **2002**, *33*, 1120.
[159] B. Vernon, M. Birdno, M. C. Preul, *US 8048407 B2* **2011**.
[160] K. F. Soodak, C. R. Brennecka, B. L. Vernon, *J. Biomed. Mater. Res., Part B* **2013**, *101B*, 1477.
[161] H. H. Bearat, B. H. Lee, B. L. Vernon, *Acta Biomater.* **2012**, *8*, 3629.
[162] B. H. Lee, H. H. Beart, V. Cheng, R. Mclemore, S. A. Robb, Z. Cui, A. Dovigi, B. L. Vernon, *J. Biomater. Sci., Polym. Ed.* **2013**, *24*, 1575.
[163] F. Mottu, D. A. Rüfenacht, A. Laurent, E. Doelker, *Biomaterials* **2002**, *23*, 121.
[164] K. P. Walsh, *Pediatr. Cardiol.* **2005**, *26*, 275.
[165] J. S. Pollak, R. I. White, *J. Vasc. Interventional Radiol.* **2001**, *12*, 907.
[166] W. Wei, J. Yang, Z. Zhang, Y. Dai, W. Li, X. Wu, H. Dai, *ACS Appl. Polym. Mater.* **2022**, *4*, 8847.
[167] Y. S. Wong, A. V. Salvekar, K. D. Zhuang, H. Liu, W. R. Birch, K. H. Tay, W. M. Huang, S. S. Venkatraman, *Biomaterials* **2016**, *102*, 98.
[168] M. Peuster, *Biomaterials* **2003**, *24*, 4057.
[169] J. Wang, J. Luo, R. Kunkel, M. Saha, B. N. Bohnstedt, C.-H. Lee, Y. Liu, *Mater. Lett.* **2019**, *250*, 38.
[170] S. A. Pineda-Castillo, J. Luo, H. Lee, B. N. Bohnstedt, Y. Liu, C.-H. Lee, *Adv. Eng. Mater.* **2021**, *23*, 2100322.
[171] G. Wang, C. Gao, B. Xiao, J. Zhang, X. Jiang, Q. Wang, J. Guo, D. Zhang, J. Liu, Y. Xie, C. Shu, J. Ding, *Regener. Biomater.* **2022**, *9*, rbac049.
[172] H. Zhang, W. Zhang, H. Qiu, G. Zhang, X. Li, H. Qi, J. Guo, J. Qian, X. Shi, X. Gao, D. Shi, D. Zhang, R. Gao, J. Ding, *Adv. Healthcare Mater.* **2022**, *11*, 2201740.
[173] Y. Shen, W. Zhang, Y. Xie, A. Li, X. Wang, X. Chen, Q. Liu, Q. Wang, G. Zhang, Q. Liu, J. Liu, D. Zhang, Z. Zhang, J. Ding, *Biomaterials* **2021**, *279*, 121208.
[174] Q. Wang, X. Yu, X. Chen, J. Gao, D. Shi, Y. Shen, J. Tang, J. He, A. Li, L. Yu, J. Ding, *ACS Appl. Mater. Interfaces* **2022**, *14*, 24197.

Hasan Hüseyin Karadeli received his MD from Ankara University, Department of Medical Faculty. He currently works as Professor at Istanbul Medeniyet University, Department of Medical Faculty. His research interests include serebrovascular disease, endovascular neuro-interventions. He is the author of 40 publications in peer-reviewed journals, 3 book chapters and 20 conference presentations. He has an h-index of 10 with 358 citations.

Emel Kuram received her Ph.D. from Gebze Technical University, Department of Mechanical Engineering. She currently works as an associate professor at Gebze Technical University, Department of Mechanical Engineering. Her research interests include polymeric materials, their processing into products, their characterization, and their medical applications. She is the author of 46 publications in peer-reviewed journals, 10 book chapters, and 18 conference presentations. She has an h-index of 18 with 1353 citations (Web of Science).